

Chapter 2

Digital Passband Modulation over AWGN Channels

The memoryless additive white Gaussian noise (AWGN) channel or simply Gaussian channel is the most important model of a discrete channel, usually used to calculate the performance of coding and modulation methods. Further important models representing fading channels are also based on the Gaussian channel and will be covered in Section 2.2.

Section 2.1 will introduce the 2-dimensional AWGN channel for passband modulation as a generalization of the 1-dimensional AWGN channel for baseband signaling discussed in Chapter 1. The basic principle of coherent communication and the Nyquist rate as well as the link budget analysis will be discussed in detail in Section 2.2. The most important 1- and 2-dimensional modulation methods ASK (Amplitude Shift Keying), PSK (Phase Shift Keying) and QAM (Quadrature Amplitude Modulation) will be described in Section 2.3, and in Section 2.4 we will derive various bounds to calculate the error probability of uncoded signaling. The performance of the modulation methods are compared by considering the symbol-error rate over the signal-to-noise ratio. In particular the asymptotic behaviour is discussed in Section 2.5.

In this book there are another two chapters based on the principles of uncoded high-level modulation schemes; in Chapter 3 we will determine the channel capacity of ASK, PSK and QAM over the AWGN channel, and in Chapter 11 we will consider a joint optimization of error-control codes and high-level modulation schemes which is known as trellis coded modulation (TCM).

2.1 One- and Two-Dimensional AWGN Channels

In this section the properties of the 1- and 2-dimensional AWGN channels are summarized and the 2-dimensional channel is described by complex numbers, which will make the definition of the passband modulation methods in the next

but one section much easier. In the next section we will deliver some more profound proofs and details for the calculation of the noise power and the link budget as well as for the Nyquist rate.

For baseband signaling only 1-dimensional real-valued signals occur, however, for passband signaling 2-dimensional modulation methods and 2-dimensional signal constellations are relevant. For each channel use, one modulation symbol (also called signal point or simply signal) consisting of two real values $x = (x_I, x_Q) \in \mathcal{A}_{\text{mod}}$ is transmitted and one symbol consisting of two real values $y = (y_I, y_Q) \in \mathcal{A}_{\text{dem}}$ is received. The formal description is simplified, if x and y are not conceived as real 2-dimensional vectors but as complex numbers according to (1.2.3)

$$x = x_I + jx_Q = |x| \cdot e^{j\varphi} \in \mathcal{A}_{\text{mod}} \subset \mathbb{C}, \quad (2.1.1)$$

where I and Q denote inphase and quadrature phase components. The components $x_I = \text{Re}(x)$ and $x_Q = \text{Im}(x)$ are called real and imaginary parts of x , and $|x| > 0$ is the absolute value. The phase (also called angle) φ is infinitely multiple-valued, since every rotation about 2π leads to the same image point. The principal value of the phase is either $\varphi \in [0, 2\pi]$ or $\varphi \in [-\pi, \pi]$. The two representations of x in (2.1.1) are related by

$$\begin{aligned} x_I &= |x| \cdot \cos(\varphi) \\ x_Q &= |x| \cdot \sin(\varphi) \end{aligned} \quad (2.1.2)$$

and

$$\begin{aligned} |x| &= \sqrt{x \cdot x^*} = \sqrt{x_I^2 + x_Q^2} \\ \varphi &= \begin{cases} \arctan(x_Q/x_I) & \text{if } x_I \geq 0 \\ \arctan(x_Q/x_I) + \pi & \text{if } x_I \leq 0 \end{cases}, \end{aligned} \quad (2.1.3)$$

where $x^* = x_I - jx_Q$ denotes the conjugate complex number to $x = x_I + jx_Q$. Note that the phase φ is continuous at $x = 0$ because of $\arctan(+\infty) = \pi/2 = \arctan(-\infty) + \pi$.

The energy per modulation symbol is defined as $E_s = E(|x|^2) = E(x_I^2 + x_Q^2)$, see (2.3.1) for more details.

For passband modulation schemes, Definition 1.3 is extended for the 2-dimensional AWGN. For each channel use, the random variable $\nu = \nu_I + j\nu_Q$ representing the noise is added to the transmitted modulation symbol $x = x_I + jx_Q \in \mathcal{A}_{\text{mod}} \subset \mathbb{C}$. The result is the received symbol $y = x + \nu$, which is again denoted $y = y_I + jy_Q \in \mathcal{A}_{\text{dem}} = \mathbb{C}$, where obviously $y_I = x_I + \nu_I$ and $y_Q = x_Q + \nu_Q$. The noise energy in each component is still $\sigma^2 = N_0/2$ as in (1.3.13) and both noise components are statistically independent. The energy per symbol of the 2-dimensional noise is

$$E(|\nu|^2) = E(\nu_I^2 + \nu_Q^2) = \frac{N_0}{2} + \frac{N_0}{2} = N_0 = 2\sigma^2 \quad (2\text{-dimensional}). \quad (2.1.4)$$

In contrast, the noise energy per symbol for baseband signaling is only half as high, because $\sigma^2 = N_0/2$ is still the noise energy:

$$E(\nu^2) = \frac{N_0}{2} = \sigma^2 \quad (1\text{-dimensional}). \quad (2.1.5)$$

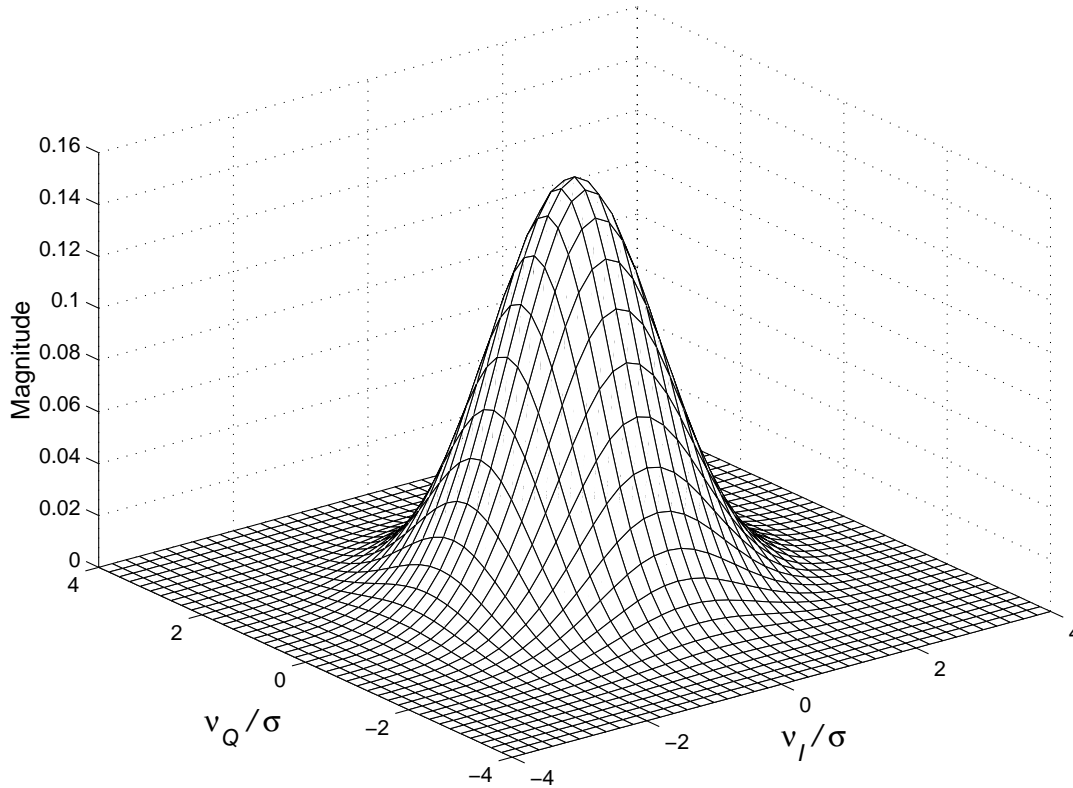


Figure 2.1. The PDF of the 2-dimensional Gaussian (normal) distribution

In the next section we will derive these results from the noise power spectral density of the AWGN channel. According to Subsection A.4.3, the probability density function (PDF) of the 2-dimensional Gaussian random variable is

$$\begin{aligned} f_{y|x}(\eta|\xi) &= \frac{1}{\pi N_0} \exp\left(-\frac{|\eta - \xi|^2}{N_0}\right) \\ &= \frac{1}{\pi N_0} \exp\left(-\frac{(\eta_I - \xi_I)^2 + (\eta_Q - \xi_Q)^2}{N_0}\right) \\ &= \frac{1}{\sqrt{\pi N_0}} \exp\left(-\frac{(\eta_I - \xi_I)^2}{N_0}\right) \cdot \frac{1}{\sqrt{\pi N_0}} \exp\left(-\frac{(\eta_Q - \xi_Q)^2}{N_0}\right) \end{aligned} \quad (2.1.6)$$

and is shown in Figure 2.1. Obviously the 2-dimensional PDF is obtained by the product of the two 1-dimensional PDFs, which is an equivalent characterization of the statistical independence of the two noise components. For further details

of the 2-dimensional Gaussian distribution we refer to Subsection A.4.3. The transition probabilities of sequences of length n have the form

$$P(\mathbf{y}|\mathbf{x}) = (\pi N_0)^{-n} \cdot \exp\left(-\frac{1}{N_0} \|\mathbf{y} - \mathbf{x}\|^2\right), \quad (2.1.7)$$

where $\|\mathbf{y} - \mathbf{x}\|$ denotes the Euclidean norm of the difference vector which is the same as the Euclidean distance d_E :

$$\begin{aligned} d_E(\mathbf{x}, \mathbf{y}) = \|\mathbf{x} - \mathbf{y}\| &= \sqrt{\sum_i |x_i - y_i|^2} \\ &= \sqrt{\sum_i ((x_{i,I} - y_{i,I})^2 + (x_{i,Q} - y_{i,Q})^2)} \end{aligned} \quad (2.1.8)$$

$$= \sqrt{\|\mathbf{x}\|^2 + \|\mathbf{y}\|^2 - 2 \cdot \operatorname{Re}\left(\sum_i x_i y_i^*\right)}. \quad (2.1.9)$$

Especially for binary signals with $x, y \in \mathcal{A}_{\text{mod}} = \{+\sqrt{E_s}, -\sqrt{E_s}\}$, we have the relation

$$d_E(\mathbf{x}, \mathbf{y}) = \sqrt{4E_s \cdot d_H(\mathbf{x}, \mathbf{y})} \quad (2.1.10)$$

between the Euclidean distance d_E and the Hamming distance d_H .

2.2 A Closer Look at the AWGN Channel with Coherent Communication

In this section we will discuss the basics of coherent passband communication in detail and derive an exact model of the 2-dimensional AWGN channel. This will also lead us to the exact proof of the statements (2.1.4) and (2.1.5) for the noise energy. Readers who are not interested in these derivations and discussions may skip this section without any disadvantage. The basic relations between the algebra of convolutions and Fourier transforms are expected to be known. For a discussion of these topics we refer to appropriate textbooks such as, for example, [6, 56, 102, 114].

2.2.1 Coherent Passband Communication and the Equivalent Discrete AWGN Channel Model

The basic model of a coherent passband communication with linearly modulated signals is shown in the top half of Figure 2.2 and the corresponding modeling by an equivalent 2-dimensional low-pass AWGN channel is in the lower half of the figure. In this subsection we will show the recovering of the desired signal

in the receiver. In the next subsection we will derive the Nyquist rate, i.e., the maximum symbol rate for which there are no intersymbol interferences. In the next but one subsection we will examine the noise energy of the AWGN channel models, and prove that $E(v_i^2) = N_0/2$ for baseband and $E(v_{i,I}^2) = E(v_{i,Q}^2) = N_0/2$ for passband signaling, if ideally $\Phi_{n,n}(f) = N_0/2$ with $-\infty < f < +\infty$ is assumed for the noise power spectral density. Finally, in the last subsection the noise energy and the link budget will be directly calculated from the physical parameters of the transmitter and the receiver.

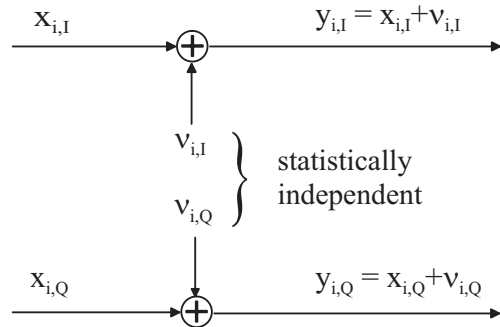
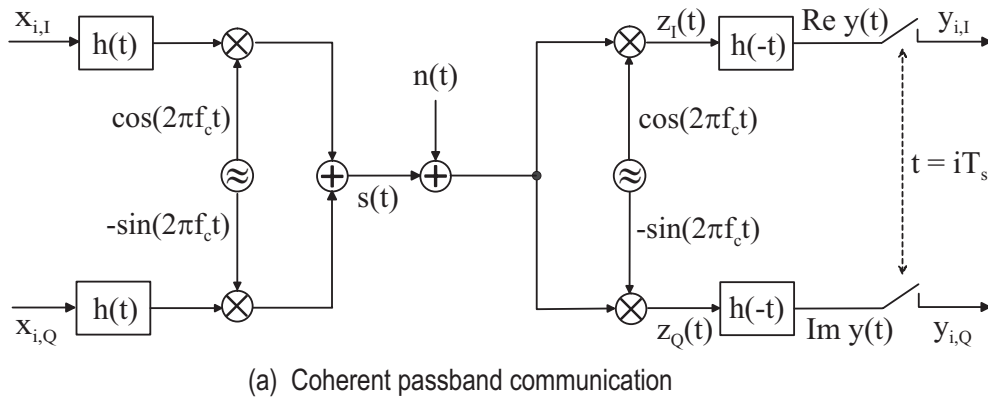


Figure 2.2. Coherent passband communication and the equivalent discrete AWGN channel model

The transmitted values $x_i = x_{i,I} + jx_{i,Q}$ in Figure 2.2 have the energy $E_s = E(|x_i|^2)$, and $x_{i,I}$ and $x_{i,Q}$ are statistically independent. Let $h(t)$ denote the real-valued transmitter filter and $H(f)$ the system transfer function. They are related by $h(t) \circ \bullet H(f)$ where the symbol $\circ \bullet$ denotes the Fourier transform.

Another Fourier relation

$$\begin{aligned} \varphi_{h,h}(t) &= h(t) \star h(-t) = \int_{-\infty}^{\infty} h(\tau)h(\tau+t) d\tau \\ &\quad \circ \\ \Phi_{h,h}(f) &= |H(f)|^2 \end{aligned} \quad (2.2.1)$$

describes the *deterministic autocorrelation function* $\varphi_{h,h}(t)$ of the transmitter filter and the corresponding Fourier transform $\Phi_{h,h}(f)$. Sometimes $\Phi_{h,h}(f)$ is also called the *energy spectral density* [128]. Furthermore, a normalization to

$$\varphi_{h,h}(0) = \int_{-\infty}^{\infty} h(t)^2 dt = \int_{-\infty}^{\infty} \Phi_{h,h}(f) df = \begin{cases} 1 & \text{baseband channel} \\ 2 & \text{passband channel} \end{cases} \quad (2.2.2)$$

is required to guarantee two properties for baseband and passband signals. Firstly, E_s is also the energy per symbol period with the duration T_s of the transmitted signal $s(t)$, see (2.2.7) for passband and (2.2.11) for baseband signaling. Secondly, at the sampling times after the receiver filter the received signal $y(t)$ is obtained as the sum of the transmitted symbols and the noise samples, i.e., $y(lT_s) = x_l + \text{noise}$, see (2.2.10) for passband and (2.2.12) for baseband signaling. By the way, the equality of the two integrals in (2.2.2) is also called Parseval's theorem. Finally, the *Nyquist criterion*

$$\varphi_{h,h}(lT_s) = 0 \quad \text{for } l \in \mathbb{Z}, l \neq 0, \quad (2.2.3)$$

which is still to be derived in Subsection 2.2.2, must also be satisfied.

(A) Signaling at passband. According to Figure 2.2(a) the transmitted signal with the carrier frequency f_c has the form

$$\begin{aligned} s(t) &= \cos(2\pi f_c t) \cdot \left[\overbrace{h(t) \star \sum_i x_{i,I} \delta(t - iT_s)}^{= x_I(t)} \right] \\ &\quad - \sin(2\pi f_c t) \cdot \left[\overbrace{h(t) \star \sum_i x_{i,Q} \delta(t - iT_s)}^{= x_Q(t)} \right] \end{aligned} \quad (2.2.4)$$

$$\begin{aligned} &= \text{Re} \left(e^{j2\pi f_c t} \cdot \underbrace{\sum_i x_i h(t - iT_s)}_{= x(t)} \right), \\ &= x_I(t) + jx_Q(t) \end{aligned} \quad (2.2.5)$$

where $\delta(t)$ denotes the delta Dirac function and T_s denotes the duration of a modulation symbol, so $r_s = 1/T_s$ is the symbol rate. During the transmission

white Gaussian noise $n(t)$, whose stochastic representation is given in Subsection 2.2.3, is added to the transmitted signal. The relation $x(t) = a(t)e^{j\varphi(t)}$ with $a(t) > 0$ as given in (2.1.1) leads to the representation

$$s(t) = a(t) \cdot \cos(2\pi f_c t + \varphi(t)), \quad (2.2.6)$$

where $x(t)$ is called the *complex envelope*, $a(t)$ is the *envelope* and $\varphi(t)$ is the *phase*.

The statistical independence of $x_{i,I} = \text{Re}(x_i)$ and $x_{i,Q} = \text{Im}(x_i)$ as well as the statistical independence of x_i and x_l for $i \neq l$ imply that the energy of the transmitted signal per symbol period is

$$\begin{aligned} \int_0^{T_s} E(s^2(t)) dt &= \int_0^{T_s} \sum_i \left(\cos^2(2\pi f_c t) E(x_{i,I}^2) + \sin^2(2\pi f_c t) E(x_{i,Q}^2) \right) h^2(t - iT_s) dt \\ &= \frac{E_s}{2} \cdot \int_0^{T_s} \sum_i h^2(t - iT_s) dt = \frac{E_s}{2} \cdot \int_{-\infty}^{\infty} h^2(t) dt \\ &= \frac{E_s}{2} \cdot \varphi_{h,h}(0) = E_s, \end{aligned} \quad (2.2.7)$$

so the energy of the transmitted signal $s(t)$ per symbol period and the energy or variance of the discrete symbols x_i are identical.

An ideal *coherent receiver* is expected to have exact knowledge of the carrier frequency f_c and the sampling times $t = iT_s$. The optimum receiver is characterized by a receiver filter which is designed to provide the maximum signal-to-noise power ratio at its output. Such a filter is referred to as a *matched filter*, and it is simply realized by the time reverse $h(-t)$ of the transmitter filter, see Problem 2.1 or for example [114, 128]. In other words, the receiver filter $h(-t)$ is “matched” to the pulse-shaping transmitter filter $h(t)$. To simplify matters, we will assume a non-causal receiver filter, so that the representation of the communication system is not further complicated by delays. The signal after the receiver filter in the two branches is combined to a complex-valued signal $y(t)$:

$$\begin{aligned} y(t) &= h(-t) \star \left(\cos(2\pi f_c t) \cdot (s(t) + n(t)) \right) \\ &\quad + jh(-t) \star \left(-\sin(2\pi f_c t) \cdot (s(t) + n(t)) \right) \\ &= h(-t) \star \left(e^{-j2\pi f_c t} s(t) \right) + \underbrace{h(-t) \star \left(e^{-j2\pi f_c t} n(t) \right)}_{= \nu(t)}. \end{aligned} \quad (2.2.8)$$

The following trigonometric identities

$$\begin{aligned} 2 \cos(A) \cos(B) &= \cos(A - B) + \cos(A + B), \\ 2 \sin(A) \sin(B) &= \cos(A - B) - \cos(A + B), \\ 2 \sin(A) \cos(A) &= \sin(A - B) + \sin(A + B) \end{aligned} \quad (2.2.9)$$

lead to

$$\begin{aligned}
e^{-j2\pi f_c t} s(t) &= \left(\cos(2\pi f_c t) - j \sin(2\pi f_c t) \right) \\
&\quad \cdot \left(\cos(2\pi f_c t) x_I(t) - \sin(2\pi f_c t) x_Q(t) \right) \\
&= \frac{1}{2} \cdot \left[x_I(t) + j x_Q(t) \right. \\
&\quad \left. + \left(\cos(2\pi 2f_c t) - j \sin(2\pi 2f_c t) \right) x_I(t) \right. \\
&\quad \left. - \left(\sin(2\pi 2f_c t) + j \cos(2\pi 2f_c t) \right) x_Q(t) \right].
\end{aligned}$$

The low-pass filtering with $h(t)$ easily suppresses all signal frequencies at the double carrier frequency $2f_c$ leaving only the signal

$$\begin{aligned}
y(t) &= \frac{1}{2} \cdot \left[h(-t) \star (x_I(t) + j x_Q(t)) \right] + \nu(t) \\
&= \frac{1}{2} \cdot \left[h(-t) \star \sum_i x_i h(t - iT_s) \right] + \nu(t) \\
&= \frac{1}{2} \cdot \sum_i x_i \varphi_{h,h}(t - iT_s) + \nu(t).
\end{aligned}$$

Thus for ideal sampling at times $t = lT_s$ with $l \in \mathbb{Z}$ and a satisfied Nyquist criterion (2.2.3) we obtain the transmitted symbols x_l with a superimposition by the noise:

$$\begin{aligned}
y_l = y(lT_s) &= y_{l,I} + j y_{l,Q} \\
&= \frac{1}{2} \cdot \left[x_l \underbrace{\varphi_{h,h}(lT_s)}_{=2} + \sum_{i \neq l} x_i \underbrace{\varphi_{h,h}(lT_s - iT_s)}_{=0} \right] + \nu(lT_s) \\
&= x_l + \nu(lT_s). \tag{2.2.10}
\end{aligned}$$

If the Nyquist criterion (2.2.3) was not satisfied, x_l would not only be superimposed by the noise samples but also by the previously transmitted symbols (and also by the following transmitted symbols because of the presumed non-causality), which are weighted with the values $\varphi_{h,h}(\pm T_s), \varphi_{h,h}(\pm 2T_s), \dots$. However, these intersymbol interferences can all be nullified with ideal sampling, if the transmitter and receiver filters are properly designed as described in the next subsection.

(B) Signaling at baseband. Here the matter is much simpler. In Figure 2.2 $f_c = 0$, so that the lower branch as well as all multiplications with $\cos(2\pi f_c t)$ and $\sin(2\pi f_c t)$ are dropped. Similar to (2.2.7), for the energy of the transmitted

signal per symbol period,

$$\begin{aligned} \int_0^{T_s} E(s^2(t)) dt &= \int_0^{T_s} \sum_i E(x_i^2) h^2(t - iT_s) dt = E_s \int_{-\infty}^{\infty} h^2(t) dt \\ &= E_s \cdot \varphi_{h,h}(0) = E_s. \end{aligned} \quad (2.2.11)$$

For the received signal after the matched filter,

$$\begin{aligned} y(t) &= h(-t) \star \left[h(t) \star \sum_i x_i \delta(t - iT_s) + n(t) \right] \\ &= \sum_i x_i \varphi(t - iT_s) + \underbrace{h(-t) \star n(t)}_{= \nu(t)} \\ &= x_l \cdot \underbrace{\varphi_{h,h}(lT_s)}_{=1} + \sum_{i \neq l} x_i \underbrace{\varphi_{h,h}(lT_s - iT_s)}_{=0} + \nu(lT_s) \\ &= x_l + \nu(lT_s) \end{aligned} \quad (2.2.12)$$

for sampling at times $t = lT_s, l \in \mathbb{Z}$.

2.2.2 The Nyquist Criterion for Intersymbol Interference-Free Communication

In (2.2.3) the Nyquist criterion $\varphi_{h,h}(lT_s) = 0$ for all $l \in \mathbb{Z}, l \neq 0$ was presupposed. In this subsection we attempt to determine the shape of pulses that satisfy this criterion of no intersymbol interference. In the course of this we will obtain a connection between the symbol rate $r_s = 1/T_s$ and the bandwidth W .

It is apparent that the Nyquist criterion (2.2.3) on the autocorrelation function is satisfied, if and only if there is equality in the time-domain equation

$$\begin{aligned} \varphi_{h,h}(0)\delta(t) &= \sum_i \varphi_{h,h}(iT_s)\delta(t - iT_s) \\ &= \varphi_{h,h}(t) \star \sum_i \delta(t - iT_s) \\ &\quad \circ \\ \varphi_{h,h}(0) &= \Phi_{h,h}(f) \cdot \frac{1}{T_s} \sum_i \delta\left(f - \frac{i}{T_s}\right) \\ &= \frac{1}{T_s} \sum_i \Phi_{h,h}\left(f - \frac{i}{T_s}\right). \end{aligned} \quad (2.2.13)$$

The last term in the frequency-domain equation is constant, if the system transfer function $G(f) = \Phi_{h,h}(f)$ is symmetric both to 0 and to $f = 0.5/T_s$, i.e.,

formally $G(f) = G(-f)$ and $G(0.5/T_s + f) = G(0.5/T_s - f)$. An important example for this is the *raised cosine filter*, whose transfer function and impulse response are shown in Figures 2.3 and 2.4. The parameter α with $0 \leq \alpha \leq 1$ is also called *rolloff factor*. A small α implies a narrow spectrum, whereas a large α causes small leading and trailing echos and therefore smaller degradations in the case of non-perfect sampling times. In most practical systems α lies between 0.1 and 0.3. Formally, for the raised cosine filter in frequency and time domain,

$$G(f) = \left\{ \begin{array}{ll} 1 & \text{if } |f| < \frac{1-\alpha}{2T_s} \\ \cos^2 \left[\frac{\pi}{2\alpha} \left(|f|T_s - \frac{1-\alpha}{2} \right) \right] & \text{if } \frac{1-\alpha}{2T_s} < |f| < \frac{1+\alpha}{2T_s} \\ 0 & \text{if } \frac{1+\alpha}{2T_s} < |f| \end{array} \right\} \quad (2.2.14)$$

$$g(t) = \frac{\sin(\pi t/T_s)}{\pi t} \cdot \frac{\cos(\alpha\pi t/T_s)}{1 - (2\alpha t/T_s)^2}$$

A simple transformation leads to further useful representations of the system

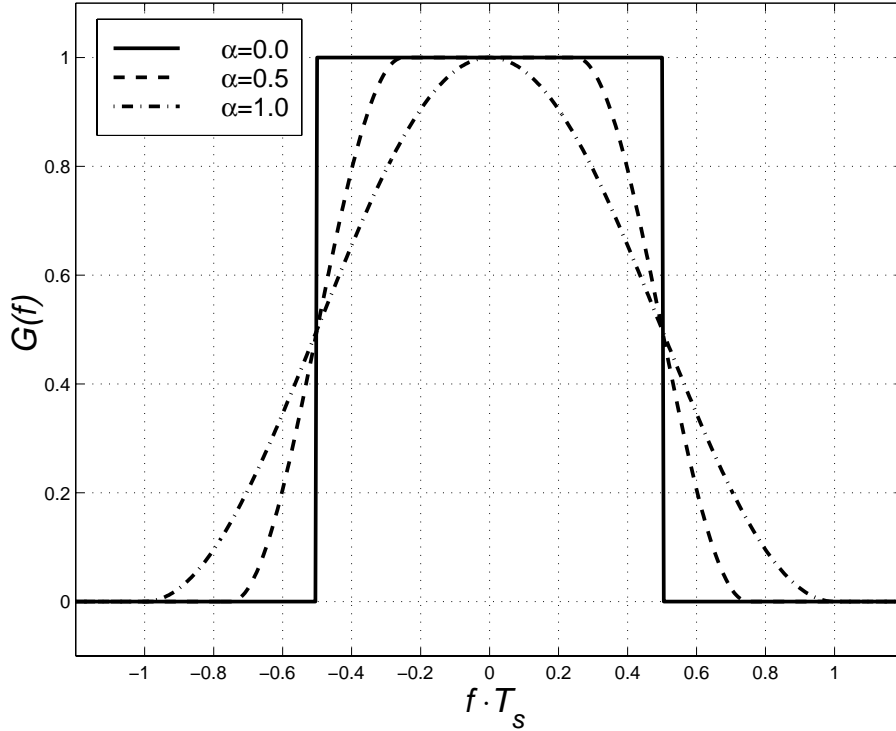


Figure 2.3. Raised cosine filter in frequency domain

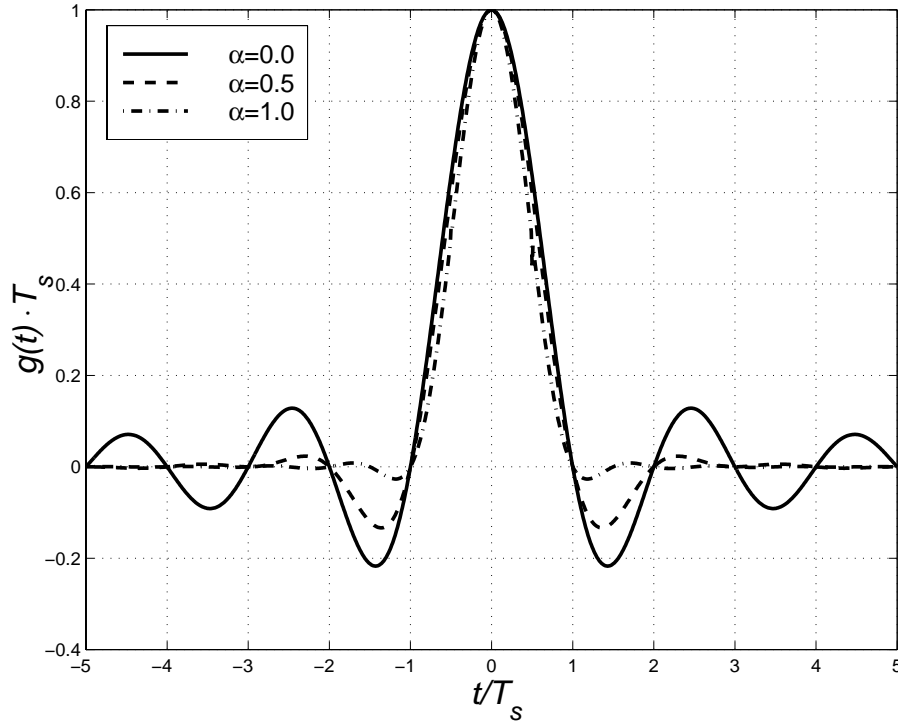


Figure 2.4. Raised cosine filter in time domain

transfer function for the range $(1 - \alpha)/(2T_s) < |f| < (1 + \alpha)/(2T_s)$:

$$\begin{aligned} \cos^2 \left[\frac{\pi}{2\alpha} \left(|f|T_s - \frac{1 - \alpha}{2} \right) \right] &= \frac{1}{2} \left(1 + \cos \left[\frac{\pi}{2\alpha} (2|f|T_s - (1 - \alpha)) \right] \right) \\ &= \frac{1}{2} \left(1 - \sin \left[\frac{\pi}{2\alpha} (2|f|T_s - 1) \right] \right). \end{aligned} \quad (2.2.15)$$

Since

$$h(t) = h(-t) \circ \bullet H(f) = \sqrt{G(f)}, \quad \varphi_{h,h}(t) = g(t), \quad (2.2.16)$$

the transmitter and receiver filters are usually also called *square root raised cosine filter*. For passband signaling, $g(t)$ and $G(f)$ have to be multiplied by 2, and $h(t)$ and $H(f)$ have to be multiplied by $\sqrt{2}$ to satisfy (2.2.2).

Particularly for $\alpha = 0$, $G(f) = 1$ if $|f| < 0.5/T_s$, and $G(f) = 0$ otherwise. Thus, $G(f) = \text{rect}(fT_s)$ is a rectangular spectrum with the corresponding impulse response

$$g(t) = \frac{\sin(\pi t/T_s)}{\pi t} = \frac{1}{T_s} \cdot \text{sinc}(t/T_s) = h(t) = \varphi_{h,h}(t),$$

where $\text{sinc}(x) = \sin(\pi x)/(\pi x)$, and $\text{rect}(x) = 1$ for $|x| < 1/2$ and $\text{rect}(x) = 0$ otherwise. Since the impulse response is unlimited on both sides, i.e., does not exactly reach zero in finite time, it has to be cut off at the edges in the time

domain for a digital implementation, which leads to a small widening of the spectrum. The larger α is, the faster $g(t)$ and $h(t)$ fade away. By the way, note the interesting relation

$$\frac{\sin(\pi t/T_s)}{\pi t} = \frac{\sin(\pi t/T_s)}{\pi t} \star \frac{\sin(\pi t/T_s)}{\pi t}$$

obtained from $\text{rect}(fT_s) = \text{rect}(fT_s) \cdot \text{rect}(fT_s)$ by inverse Fourier transform.

A further example of the satisfaction of the Nyquist criterion (2.2.3) is given by a rectangular impulse in the time domain

$$h(t) = \frac{1}{T_s} \text{rect}\left(\frac{t}{T_s}\right), \quad g(t) = \varphi_{h,h}(t) = \begin{cases} 1 - \frac{|t|}{T_s} & \text{if } |t| \leq T_s \\ 0 & \text{otherwise} \end{cases},$$

$$\begin{array}{ccc} \circ & & \circ \\ | & & | \\ \bullet & & \bullet \end{array} \quad (2.2.17)$$

$$H(f) = \text{sinc}(fT_s), \quad G(f) = \Phi_{h,h}(f) = \text{sinc}^2(fT_s).$$

The corresponding autocorrelation function is a triangular function. Since the received signal is integrated over a symbol period, the term *integrate-and-dump receiver* is also often used. Since $H(f)$ in (2.2.17) never exactly reaches zero, the bandwidth is theoretically unlimited. A cut on the spectrum required for a practical implementation then leads to slight intersymbol interferences. The example in (2.2.17) with a rectangular impulse response and the raised cosine impulse with a rectangular spectrum for $\alpha = 0$, introduced in (2.2.14), emphasizes that the product of bandwidth and symbol duration is, in theory, always infinitely large.

The bandwidth is only defined for positive frequencies. Since

$$G(f) > 0 \quad \text{only if} \quad \begin{cases} |f| < \frac{1+\alpha}{2T_s} & \text{baseband channel} \\ |f - f_c| < \frac{1+\alpha}{2T_s} & \text{passband channel} \end{cases}, \quad (2.2.18)$$

the bandwidth W_α for the raised cosine impulse with $r_s = 1/T_s$ turns out to be

$$W_\alpha = r_s \cdot \begin{cases} \frac{1+\alpha}{2} & \text{baseband channel} \\ 1+\alpha & \text{passband channel} \end{cases}. \quad (2.2.19)$$

Trivially the minimum bandwidth $W = W_0$ results for $\alpha = 0$, this is also referred to as the *Nyquist bandwidth*. Hence, the maximum number r_s of modulation symbols to be transmitted per second is limited to $r_s \leq 2W$ for baseband signaling or $r_s \leq W$ for passband signaling, given the requirement of no intersymbol interference for a channel with noise but without any signal distortions.

The Nyquist rate is also related to the *Shannon sampling Theorem*, introduced to communication theory in 1949 by C.E.Shannon. This famous theorem

states that a baseband band-limited signal $s(t)$ of bandwidth W is uniquely represented by samples of $s(t)$, taken at a rate of at least double the bandwidth, i.e., at $r_{\text{samp}} = 1/T_{\text{samp}} \geq 2W$ samples per second. The signal can be reconstructed from its samples by use of the interpolation formula

$$s(t) = \sum_i s(iT_{\text{samp}}) \cdot \text{sinc}\left(\frac{t - iT_{\text{samp}}}{T_{\text{samp}}}\right), \quad (2.2.20)$$

where $\text{sinc}(x) = \sin(\pi x)/(\pi x)$. Sampling below the Nyquist rate results in frequency aliasing. The proof is contained in nearly every textbook on digital communications.

2.2.3 Representation of Passband and Baseband Noise

In Figure 2.2, $n(t)$ represents the continuous-time noise signal, also called the *input noise* to the receiver. The objective of this subsection is to determine the *output noise* $\nu_l = \nu(lT_s)$ of the demodulator as defined in (2.2.10) for passband and (2.2.12) for baseband signaling from the properties of the input noise $n(t)$. While $E(n^2(t))$ has the unit of instantaneous power, $E(\nu_l^2)$ is the average energy per symbol period.

The primary spectral characteristic of thermal noise is that its *power spectral density* (also called *power density spectrum*) $\Phi_{n,n}(f)$ is constant over all frequencies of interest. In other words, a thermal noise source emanates an equal amount of noise power per unit bandwidth at all interesting frequencies – typically from dc to about 10^{12} Hz [128]. Therefore, a simple model for thermal noise is the ideal AWGN channel with a noise power spectral density which is constant over all frequencies (the term *white* in the AWGN abbreviation refers to the *constant* spectral density):

$$\begin{aligned} \Phi_{n,n}(f) &= \frac{N_0}{2}, \quad -\infty < f < +\infty \\ &\quad \bullet \\ &\quad \circ \\ \varphi_{n,n}(t) &= \frac{N_0}{2} \cdot \delta(t). \end{aligned} \quad (2.2.21)$$

The *autocorrelation function* $\varphi_{n,n}(t)$ is given by the inverse Fourier transform of the power spectral density, which is also known as the *Wiener-Khintchine relation*. For white noise, $\varphi_{n,n}(t)$ turns out to be a delta Dirac function weighted by the factor $N_0/2$, where N_0 is called *one-sided* and $N_0/2$ is called *two-sided noise power density*. Generally, $\varphi_{n,n}(t) = E(n(t+\tau)n(\tau))$, where the autocorrelation function is independent of τ , since $n(t)$ is presupposed to be a stationary stochastic process.

According to (2.2.21), formally, the noise power is not finite, because $E(n^2(t)) = \varphi_{n,n}(0) = \int_{-\infty}^{\infty} \Phi_{n,n}(f) df = \infty$. However, since this, of course,

is not physically realizable, and the properties of the noise for frequencies outside of the spectrum of the transmitted signal are practically irrelevant, we can simply assume a spectral limitation of the noise, which then also leads analytically to a finite noise power. This spectral limitation is, of course, guaranteed in practice by the receiver filter, whereby all noise frequencies outside of the spectrum of the transmitted signal are suppressed.

All statements in this subsection so far are not only valid for baseband but also for passband signaling. We will now treat these two cases separately.

(A) Signaling at passband. For a comprehensive analysis of passband Gaussian noise we refer to [103, 114, 152]. Here we will examine a simpler model. According to (2.2.8), $\nu(t) = h(-t) \star z(t)$ with $z(t) = e^{-j2\pi f_c t} n(t)$, thus for the real and imaginary parts of the noise,

$$\begin{aligned}\nu_I(t) &= h(-t) \star \underbrace{(\cos(2\pi f_c t) n(t))}_{= z_I(t)} = \int_{-\infty}^{\infty} h(\tau - t) \cos(2\pi f_c t) n(t) d\tau, \\ \nu_Q(t) &= h(-t) \star \underbrace{(-\sin(2\pi f_c t) n(t))}_{= z_Q(t)} = \int_{-\infty}^{\infty} h(\tau - t) \sin(2\pi f_c t) n(t) d\tau.\end{aligned}\tag{2.2.22}$$

So with $E(n(\tau)n(\tau')) = N_0/2 \cdot \delta(\tau - \tau')$ we obtain

$$\begin{aligned}E(\nu_I^2(t)) &= \int_{-\infty}^{\infty} \int_{-\infty}^{\infty} h(\tau - t) h(\tau' - t) \cos(2\pi f_c \tau) \cos(2\pi f_c \tau') E(n(\tau)n(\tau')) d\tau d\tau' \\ &= \frac{N_0}{2} \cdot \int_{-\infty}^{\infty} h^2(\tau - t) \cos^2(2\pi f_c \tau) d\tau.\end{aligned}$$

Obviously, we can use the approximation $\cos^2(2\pi f_c \tau) \approx 1/2$, because the function $\cos^2(2\pi f_c \tau)$ oscillates at high-frequency in comparison to $h(t)$. So with (2.2.2) this finally leads to

$$E(\nu_I^2(t)) = \frac{N_0}{4} \cdot \int_{-\infty}^{\infty} h^2(\tau) d\tau = \frac{N_0}{4} \cdot \underbrace{\varphi_{h,h}(0)}_{= 2} = \frac{N_0}{2}.\tag{2.2.23}$$

It is obvious that also $E(\nu_Q^2(t)) = N_0/2$. Furthermore with the previous methods

$$E(\nu_I(t)\nu_Q(t)) = \frac{N_0}{2} \cdot \int_{-\infty}^{\infty} h^2(\tau - t) \underbrace{\cos(2\pi f_c \tau) \sin(2\pi f_c \tau)}_{= \sin(4\pi f_c \tau)/2 \approx 0} d\tau = 0,\tag{2.2.24}$$

thus $\text{Re}(\nu_I)$ and $\text{Im}(\nu_I)$ are statistically independent.

(B) Signaling at baseband. According to (2.2.12), $\nu(t) = h(-t) \star n(t)$ for the noise after the receiver filter, thus for the power spectral density and the autocorrelation function

$$\begin{aligned} \Phi_{\nu,\nu}(f) &= \Phi_{n,n}(f) \cdot |H(f)|^2 = \frac{N_0}{2} |H(f)|^2 \\ &\quad \downarrow \\ \varphi_{\nu,\nu}(f) &= \varphi_{n,n}(t) \star \varphi_{h,h}(t) = \frac{N_0}{2} \varphi_{h,h}(t). \end{aligned} \quad (2.2.25)$$

Finally, with (2.2.2),

$$E(\nu^2(t)) = \varphi_{\nu,\nu}(0) = \frac{N_0}{2} \cdot \underbrace{\varphi_{h,h}(0)}_{=1} = \frac{N_0}{2}. \quad (2.2.26)$$

(C) Summary of passband and baseband signaling. The average signal power for passband as well as for baseband signaling, according to (2.2.7) and (2.2.11), is

$$S = \int_0^{T_s} E(s^2(t)) dt = E_s \cdot r_s = E_b \cdot r_b, \quad (2.2.27)$$

where E_s and E_b denote the signal energy per symbol and per information bit, and r_s and r_b denote the symbol rate of the channel (or baud rate) and the bit rate of the information source, respectively. From Section 1.4 we recall the relations $E_s = RM \cdot E_b$ and $r_s = r_b/(RM)$ for a code rate of R and 2^M -ary modulation.

The noise power N is the product of the bandwidth and the one-sided power spectral density,

$$N = N_0 \cdot W = \left\{ \begin{array}{ll} N_0 \cdot r_s/2 & \text{baseband channel} \\ N_0 \cdot r_s & \text{passband channel} \end{array} \right\}. \quad (2.2.28)$$

So for the signal-to-noise power ratio,

$$\frac{S}{N} = \left\{ \begin{array}{ll} 2E_s/N_0 & \text{baseband channel} \\ E_s/N_0 & \text{passband channel} \end{array} \right\}. \quad (2.2.29)$$

For passband channels, $E(|\nu_i|^2) = E(\nu_{i,I}^2 + \nu_{i,Q}^2) = N_0/2 + N_0/2 = N_0$. Thus for baseband as well as for passband signaling generally

$$\frac{E(|x_i|^2)}{E(|\nu_i|^2)} = \frac{S}{N}. \quad (2.2.30)$$

In other words, the ratio of signal-to-noise energies per symbol period equals the signal-to-noise power ratio.

2.2.4 Link Budget of Wireless Transmission

In this subsection, we will determine the signal-to-noise ratio $E_s/N_0 = S/N$ from the physical parameters of a wireless transmission, and we presuppose a passband AWGN channel to represent the thermal noise. Many other influences have to be considered, including the distance between transmitter and receiver, the carrier frequency, the bandwidth, the antenna characteristics, maybe additional rain fading and some further details. A more detailed communication link budget analysis can be found, for example, in [128].

For the power relationship between transmitter and receiver, we assume that the transmission is not influenced by the earth's surface or other obstructing bodies. For instance, this is ideally satisfied for space communication or microwave line-of-sight communication, but not for mobile radio, of course. Let P_{Tx} be the average transmitted power in Watts, then the average received power S can be calculated from the expression

$$S = \frac{P_{Tx} \cdot G_{Tx} \cdot G_{Rx}}{L_{free} \cdot L_{rain} \cdot L_0}, \quad (2.2.31)$$

where

- G_{Tx} and G_{Rx} describe the directive *antenna gains* of transmitter and receiver antennas, respectively. The gain G can be calculated as follows from the *physical aperture area* A , given in square meters (for example $A = \pi D^2/4$ for a parabolic antenna with *diameter* D), and the *antenna efficiency factor* η (which is typically between 0.55 for a parabolic reflector and 0.75 for a horn-shaped antenna [128])

$$G = \frac{4\pi A\eta}{\lambda^2}. \quad (2.2.32)$$

The product $A\eta$ describes the *effective aperture area* of the antenna. An omnidirectional antenna with isotropic radiated power is characterized by $G_{Tx} = 1$. Only the product $P_{Tx} \cdot G_{Tx}$ rather than the single factors is relevant for the receiver, and this product is usually referred to as the *equivalent isotropic radiated power (EIRP)*.

- L_{free} describes the *path loss* or *free-space loss* which can be calculated as

$$L_{free} = \left(\frac{4\pi d}{\lambda} \right)^2, \quad (2.2.33)$$

or $L_{free,dB} = 20 \cdot \log_{10}(4\pi d/\lambda)$ in decibels, where d is the *distance between the transmitter and the receiver antenna* (also called *range*) in meters and $\lambda = c/f_c$ is the *wavelength* in meters which can be calculated from the *velocity of light* $c \approx 3 \cdot 10^8$ m/s and the *carrier frequency* f_c in Hertz. Hence, a doubling of the distance or a doubling of the carrier frequency increases the path loss by 6 dB.

- L_{rain} describes the *rain fading* which is highly dependent on the frequency range (and also on more sophisticated things like *rain zone* and *average link availability per year*). For a simple approximation, the rain fading can be assumed to be proportional to the distance with a fixed constant $L_{rain/km}$ describing the rain fading per km:

$$L_{rain} \approx d \cdot 1000 \cdot L_{rain/km}. \quad (2.2.34)$$

However, this is not *exactly* true and for a detailed analysis of rain fading we refer to [153]. An application of error-control coding in wireless microwave line-of-sight access systems with considerable influence from rain fading is presented in Section 2.2. For satellite communications, the rain fading is trivially a fixed amount and does not depend on the satellite's distance.

- L_0 represents additional implementation losses or may contain a *safety factor* (also called *link margin*, usually between 1 and 5 dB depending on the application under consideration).

The input noise power at the receiver can be calculated as follows (using some slight simplifications)

$$N = N_0 \cdot W = FKT \cdot W, \quad (2.2.35)$$

where F is the dimensionless *receiver noise figure* (typically between 5 and 8 dB), $K = 1.38 \cdot 10^{-23}$ Joule/Kelvin is the *Boltzmann constant*, $T = 290$ Kelvin is the *standard "room" temperature* and W is the bandwidth in Hertz. The noise power results in units of Watts (remember that Joule equals Watts times seconds or Watts per Hertz, i.e., $J = W \cdot s = W/Hz$). The value of T also results in an aesthetically pleasing number of $KT = 4 \cdot 10^{-21}$ or -204 dBW/Hz or -174 dBm/Hz. It should be mentioned that a doubling of the bandwidth increases the noise power by 3 dB.

Finally, we can now calculate E_s/N_0 from the physical parameters of the transmitter and the receiver,

$$\frac{E_s}{N_0} = \frac{S}{N} = \frac{P_{Tx} \cdot G_{Tx} \cdot G_{Rx}}{N \cdot L_{free} \cdot L_{rain} \cdot L_0}, \quad (2.2.36)$$

this term is called the *signal-to-noise ratio* (S/N or SNR) or *carrier power-to-noise ratio* (C/N). To guarantee a specified value of E_s/N_0 at the receiver, the minimum required transmit power, expressed in decibels, is

$$P_{Tx,dB} = \left(\frac{E_s}{N_0} \right)_{dB} + N_{dB} + L_{free,dB} + L_{rain,dB} + L_{0,dB} - G_{Tx,dB} - G_{Rx,dB} \quad (2.2.37)$$

Example 2.1. (Adopted from [151]). Consider a satellite at an altitude of $d = 800$ km transmitting to a mobile receiver at $f_c = 1.5$ GHz with a bandwidth of $W = 1$ MHz. Hence, $\lambda = 0.2$ m for the wavelength and $L_{free} = 154.0$ dB for the path loss. Rain fading does not occur at such low frequencies.

For the satellite we assume an antenna gain of $G_{Tx} = 30$ dBi and a transmit power of $P_{Tx} = 100$ W or 20 dBW, so the EIRP is 50 dBW.

For the receiver we assume an antenna gain of $G_{Rx} = 3$ dBi and a link margin of $L_0 = 6$ dB. Hence, the received signal power is $S = 20 + 30 + 3 - 154.03 - 0 - 6 = -107.0$ dBW or -77.0 dBm or $1.98 \cdot 10^{-8}$ mW. Furthermore, we assume a noise figure of 5 dB, resulting in a noise power of $N = 5 - 204 + 10 \cdot \log_{10}(10^6) = -139.0$ dBW or -109.0 dBm or $1.27 \cdot 10^{-11}$ mW.

Finally, we obtain $E_s/N_0 = S/N = -107.0 - (-139.0) = 32.0$ dB. ■

2.3 Some One- and Two-Dimensional Signal Constellations (ASK, PSK, QAM)

2.3.1 Minimum Euclidean Distance

We consider an AWGN channel with a 2^M -ary modulation alphabet or signal constellation $\mathcal{A}_{\text{mod}} = \{\xi_0, \dots, \xi_{2^M-1}\}$, and, as in Section 1.6, presuppose that the single modulation symbols or signal points occur with equal a priori probabilities $P(x = \xi_i) = P_x(\xi_i) = 2^{-M}$. Furthermore, on average the energy per encoded symbol (i.e., per channel use) is denoted

$$E_s = E(|x|^2) = \frac{1}{2^M} \cdot \sum_{i=0}^{2^M-1} |\xi_i|^2. \quad (2.3.1)$$

Figure 2.5 in the next subsection shows some 1-dimensional (ASK) and 2-dimensional (PSK, QAM) signal constellations which are normalized to the same E_s for easier comparison. The parameter

$$\Delta_0 = \min_{i,l} \frac{|\xi_i - \xi_l|}{\sqrt{E_s}} \quad (2.3.2)$$

denotes the minimum Euclidean distance between the signal points in the modulation alphabet \mathcal{A}_{mod} after normalizing to unit symbol energy $E_s = 1$. So $\Delta_0 \sqrt{E_s} = \min_{i,l} |\xi_i - \xi_l|$ is the minimum Euclidean distance in the general case. The index 0 of Δ will become clear in Chapter 11, where we will introduce further distances within the signal constellation.

(1) For 2^M -ASK (Amplitude Shift Keying), the signal constellation is

$$\mathcal{A}_{\text{mod,ASK}} = \left\{ (2i - 2^M + 1) \sqrt{\frac{3}{2^{2M} - 1} E_s} \mid i = 0, \dots, 2^M - 1 \right\} \quad (2.3.3)$$

and the minimum Euclidean distance is

$$\Delta_{0,\text{ASK}} = \sqrt{\frac{12}{2^{2M} - 1}}. \quad (2.3.4)$$

(2) For 2^M -PSK (Phase Shift Keying), the signal constellation is

$$\mathcal{A}_{\text{mod,PSK}} = \left\{ e^{j2\pi i/2^M} \sqrt{E_s} \mid i = 0, \dots, 2^M - 1 \right\} \quad (2.3.5)$$

and the minimum Euclidean distance is

$$\Delta_{0,\text{PSK}} = 2 \cdot \sin(\pi/2^M), \quad (2.3.6)$$

where $\Delta_{0,\text{PSK}}$ is obtained by elementary geometric calculations. For some small values of M , we note that $\Delta_{0,2\text{-PSK}} = 2$, $\Delta_{0,4\text{-PSK}} = \sqrt{2}$ and $\Delta_{0,8\text{-PSK}} = \sqrt{2 - \sqrt{2}}$.

(3) For 2^M -QAM (Quadrature Amplitude Modulation) the signal points are on a trellis which is why the term \mathbb{Z}^2 -*signal constellation* is often used. More precisely, this is also called $2\mathbb{Z}^2 + (1, 1)$ -*signal constellation*. In the special case of M being an even integer,

$$\mathcal{A}_{\text{mod,QAM}} = \left\{ (i + jl) \frac{\Delta_0}{2} \sqrt{E_s} \mid i, l = \pm 1, \pm 3, \dots, \pm(2^{M/2} - 1) \right\} \quad (2.3.7)$$

for the signal constellation, and

$$\Delta_{0,\text{QAM}} = \sqrt{\frac{6}{2^M - 1}} \quad (2.3.8)$$

for the minimum Euclidean distance. For example, 64-QAM emerges from an 8×8 pattern and 256-QAM from a 16×16 pattern. 32-QAM emerges from a 6×6 pattern by omitting the four corners (see also Figure 11.11?), 128-QAM emerges from a 12×12 pattern by omitting the four 2×2 subpatterns at the corners. A sphere-shaped 960-QAM constellation is shown in Figure 16.?

Table 2.1 contains a list of the minimum Euclidean distances of ASK, PSK and QAM for values of M which are relevant in practice.

Table 2.1. Minimum Euclidean distance Δ_0 in the modulation alphabet \mathcal{A}_{mod}

M	2^M	ASK	PSK	QAM
1	2	2.0000	2.0000	
2	4	0.8944	1.4142	$\sqrt{2} = 1.4142$
3	8	0.4364	0.7654	
4	16	0.2169	0.3902	$\sqrt{2/5} = 0.6325$
5	32	0.1083	0.1960	$\sqrt{2/10} = 0.4472$
6	64	0.0541	0.0981	$\sqrt{2/21} = 0.3086$
7	128	0.0271	0.0491	$\sqrt{2/41} = 0.2209$
8	256	0.0135	0.0245	$\sqrt{2/85} = 0.1534$

2.3.2 Some Examples of Signal Constellations

Figure 2.5 shows some 1- and 2-dimensional signal constellations for ASK, PSK and QAM. As already mentioned, the scale is chosen such that the symbol energy E_s is identical for the five modulation schemes. 2-PSK is the same as 2-ASK and is also called BPSK (Binary Phase Shift Keying). 4-PSK and 4-QAM are also identical and are often called QPSK (Quaternary Phase Shift Keying).

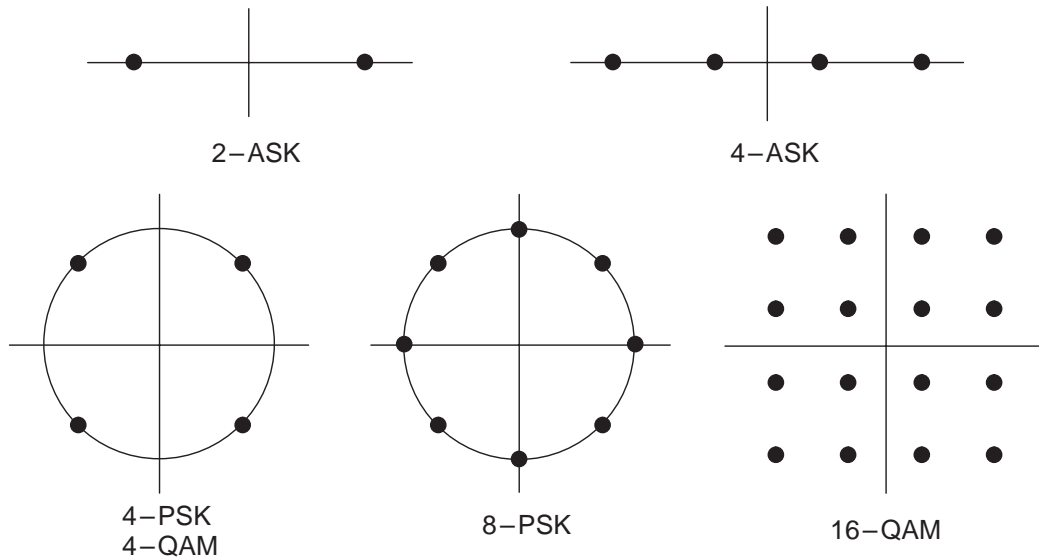


Figure 2.5. Some 1- and 2-dimensional signal constellations (ASK, PSK, QAM)

Figures 2.6, 2.7 and 2.8 show some scatter plots of received noisy signal constellations, each with a normalization of the signal energy to $E_s = 1$. There are 100 received symbols per signal point in the three Figures, i.e., 800 received values altogether for the two 8-PSK figures and 6400 received values for 64-QAM. The lines bound the decision regions, which are sectors in the case of PSK and quadratic (except for the outer regions) in the case of QAM. The ratio E_s/N_0 is mentioned at the bottom right-hand corner of each of the three figures. From the performance curves in Figure 2.10 one can see that the symbol-error rate is about 10^{-5} in Figure 2.6, about 10^{-1} in Figure 2.7 and about 10^{-11} in Figure 2.8. In Figures 2.6 and 2.7, the signal points are alternately marked as circles and crosses to distinguish adjacent sectors.

For further details of the modulation schemes we refer to according textbooks, for example [6, 56, 114, 112, 128, 151].

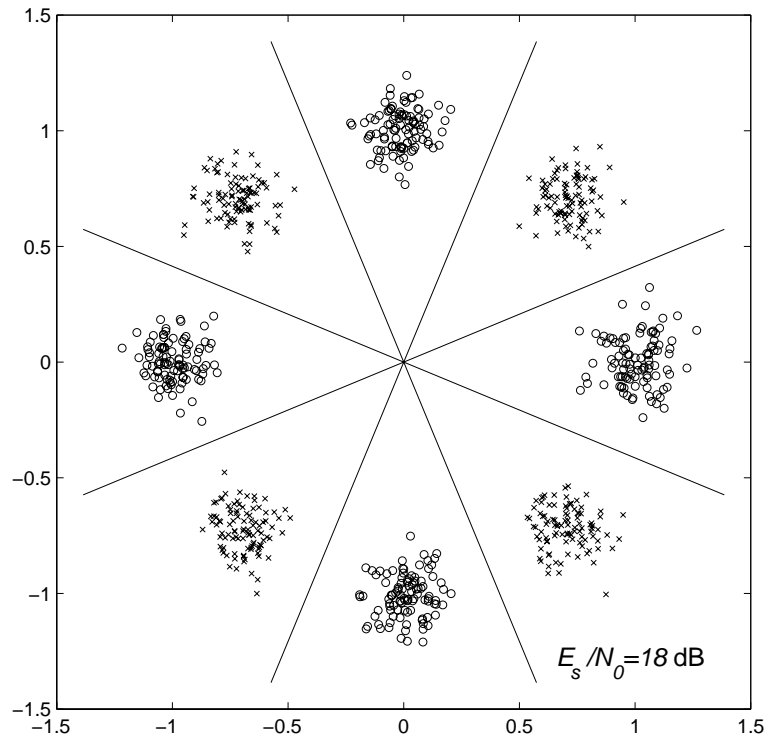


Figure 2.6. 8-PSK noisy signal constellation with high signal-to-noise ratio

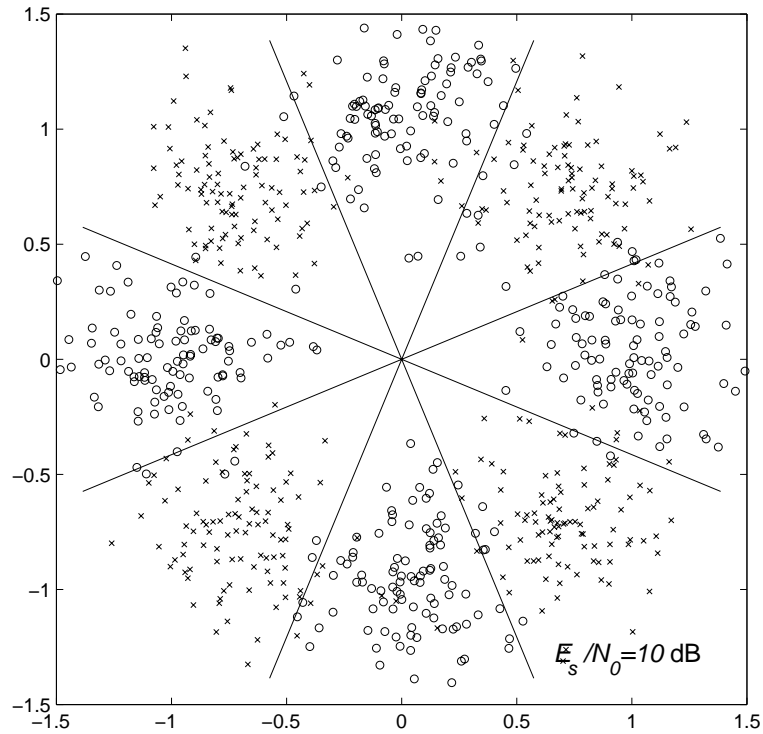


Figure 2.7. 8-PSK noisy signal constellation with low signal-to-noise ratio

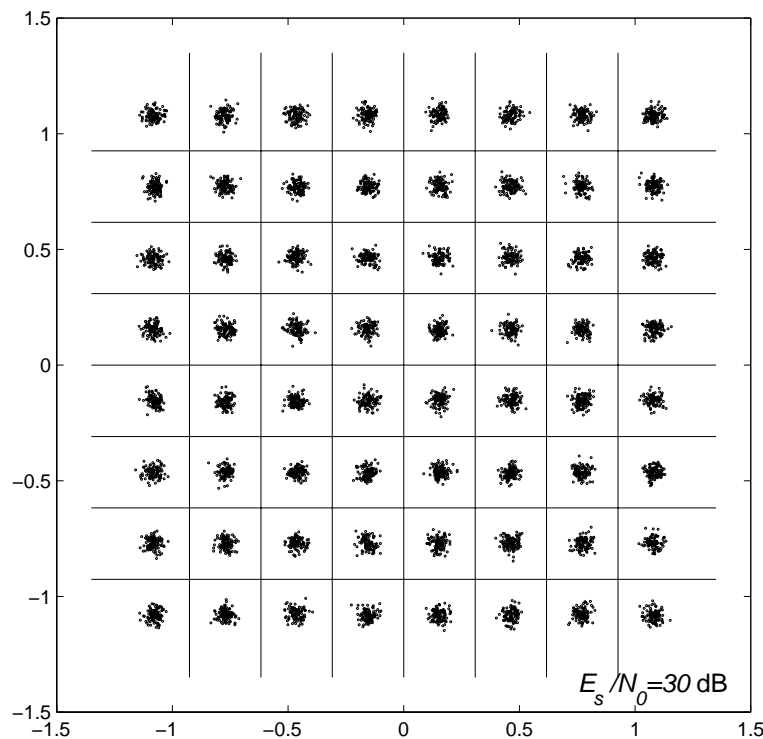


Figure 2.8. 64-QAM noisy signal constellation

2.4 Performance Analysis of Uncoded Signaling over AWGN Channels

An exact calculation of the error rate is also impossible to make for uncoded signaling, except for a few very simple modulation schemes like 2-PSK and 4-PSK. So first we will derive a generally applicable weak bound and then two specific tight bounds for PSK and QAM. These results will then be illustrated in various figures with performance curves.

2.4.1 A General Weak Bound for Arbitrary Modulation Schemes

In the following, we will approximate the error probability for arbitrary uncoded 2^M -ary modulation schemes. The decision device in the demodulator decides on $\hat{x} \in \mathcal{A}_{\text{mod}} = \mathcal{A}_{\text{dem}}$ by quantizing the received signal $y = x + \nu$. Obviously, allocations to adjacent signal points are more probable than to signal points which are further away. The symbol-error probability P_s is only slightly overestimated, if for each $|\nu| > \Delta_0/2 \cdot \sqrt{E_s}$ one error is assumed, so generally

$$P_s \leq P \left(|\nu| > \frac{\Delta_0}{2} \sqrt{E_s} \right) = \exp \left(-\frac{\Delta_0^2 E_s}{4N_0} \right). \quad (2.4.1)$$

This equality is obtained similarly to the proof of (A.4.5) in Subsection A.4.2:

$$P\left(|\nu| > \frac{\Delta_0}{2}\sqrt{E_s}\right) = \iint_{\nu_I^2 + \nu_Q^2 > \Delta_0^2 E_s / 4} \frac{1}{\pi N_0} e^{-(\nu_I^2 + \nu_Q^2)/N_0} d\nu_I d\nu_Q$$

A substitution with polar coordinates, $\nu_I = r\sqrt{N_0}\cos\varphi$, $\nu_Q = r\sqrt{N_0}\sin\varphi$ leads to the Jacobian determinant

$$\det\left(\frac{\partial(\nu_I, \nu_Q)}{\partial(r, \varphi)}\right) = \det\begin{pmatrix} \sqrt{N_0}\cos\varphi & \sqrt{N_0}\sin\varphi \\ -r\sqrt{N_0}\sin\varphi & r\sqrt{N_0}\cos\varphi \end{pmatrix} = r\sqrt{N_0}.$$

Hence, with a further substitution $u = r^2$,

$$\begin{aligned} P\left(|\nu| > \frac{\Delta_0}{2}\sqrt{E_s}\right) &= \int_{r^2 > \frac{\Delta_0^2 E_s}{4N_0}} \int_{\varphi=0}^{2\pi} \frac{r}{\pi} \cdot e^{-r^2} d\varphi dr \\ &= \int_{\frac{\Delta_0^2 E_s}{4N_0}}^{\infty} e^{-u} du = \exp\left(-\frac{\Delta_0^2 E_s}{4N_0}\right). \end{aligned}$$

So (2.4.1) is proven. If we apply the inequality (A.4.17) to this result, it leads to a lower bound, but unfortunately not to an upper bound for P_s :

$$P_s \leq \exp\left(-\frac{\Delta_0^2 E_s}{4N_0}\right) \geq 2 \cdot Q\left(\sqrt{\frac{\Delta_0^2 E_s}{2N_0}}\right). \quad (2.4.2)$$

Both terms on the right side of the inequality in (2.4.2) are shown in Figure 1.5 (with $\Delta_0 = 2$) and in Figure A.5, however, with different scaling factors.

2.4.2 A Tight Bound for PSK

Particularly for PSK, a more precise approximation of the symbol-error rate can be derived, as will be demonstrated in Figure 2.9. The correct decision region of PSK corresponds to the sector which is not hatched (i.e., the unlimited sector), whereas for the general upper bound in (2.4.1) the decision region was decreased to a sphere of radius $\Delta_0\sqrt{E_s}/2$. In Figure 2.9, \mathcal{B}_1 and \mathcal{B}_2 denote the two half-planes. The following very exact approximation of the symbol-error rate is obtained by counting the opposite double-hatched sector twice. Especially for a large E_s/N_0 , there are only seldomly received values in the double-hatched region so that the error in the following inequality is very small:

$$\begin{aligned}
P_{s,\text{PSK}} &= P(x + \nu \in \mathcal{B}_1 \cup \mathcal{B}_2) \\
&= P(x + \nu \in \mathcal{B}_1) + P(x + \nu \in \mathcal{B}_2) - P(x + \nu \in \mathcal{B}_1 \cap \mathcal{B}_2) \\
&\leq P(x + \nu \in \mathcal{B}_1) + P(x + \nu \in \mathcal{B}_2) \\
&= 2 \cdot P(x + \nu \in \mathcal{B}_1) \\
&= 2 \cdot P\left(\nu_p > \Delta_0 \sqrt{E_s}/2\right),
\end{aligned}$$

where ν_p denotes the 1-dimensional noise component, which is perpendicular to the boundary of the half-plane \mathcal{B}_1 . Since the 2-dimensional Gaussian noise is rotationally invariant (see the considerations at the end of Appendix A.4.3), ν_p as well as ν_I and ν_Q have the variance $\sigma^2 = N_0/2$. Thus

$$\begin{aligned}
P_{s,\text{PSK}} &\leq 2 \cdot P\left(\nu_p > \Delta_0 \sqrt{E_s}/2\right) \\
&= 2 \cdot P\left(\frac{\nu_p}{\sqrt{N_0/2}} > \sqrt{\frac{\Delta_0^2 E_s}{2N_0}}\right) \\
&= 2 \cdot Q\left(\sqrt{\frac{\Delta_0^2 E_s}{2N_0}}\right) = 2 \cdot Q\left(\sqrt{\frac{2E_s}{N_0}} \cdot \sin\left(\frac{\pi}{q}\right)\right). \tag{2.4.3}
\end{aligned}$$

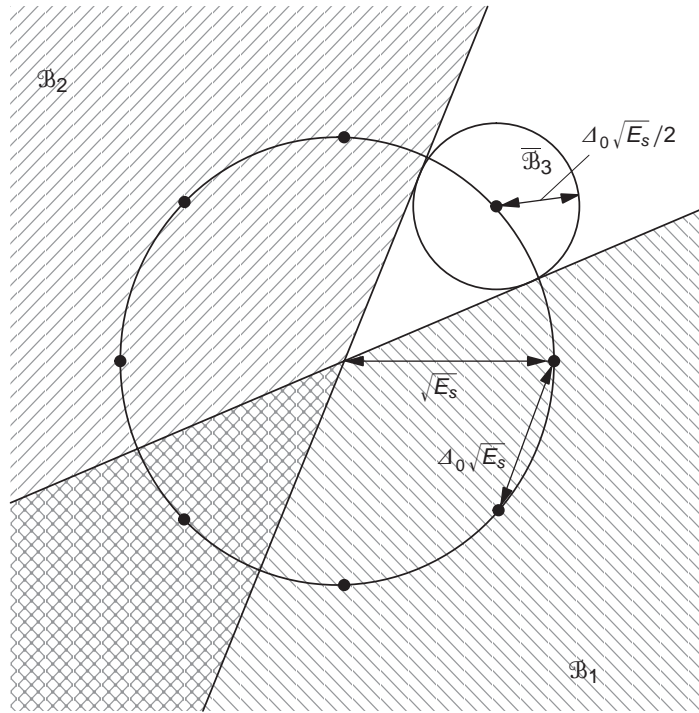


Figure 2.9. Decision regions for computing PSK symbol-error probabilities ($q = 8$)

For 4-PSK the symbol-error rate can even be calculated exactly without any approximation errors. Again we consider Figure 2.9, where the boundary lines of \mathcal{B}_1 and \mathcal{B}_2 are perpendicular to one another at $M = 2$, which results in

$$\begin{aligned}
P_{s,4\text{-PSK}} &= P(x + \nu \in \mathcal{B}_1 \cup \mathcal{B}_2) \\
&= 1 - P(x + \nu \in \overline{\mathcal{B}_1 \cup \mathcal{B}_2}) \\
&= 1 - P(x_I + \nu_I > 0 \text{ and } x_Q + \nu_Q > 0) \\
&= 1 - P(\nu_I > -x_I \text{ and } \nu_Q > -x_Q) \\
&= 1 - P\left(\nu_I > -\sqrt{E_s/2}\right)^2 \\
&= 1 - \left(1 - Q\left(\sqrt{\frac{E_s}{N_0}}\right)\right)^2 \\
&= Q\left(\sqrt{\frac{E_s}{N_0}}\right) \cdot \underbrace{\left[2 - Q\left(\sqrt{\frac{E_s}{N_0}}\right)\right]}_{\approx 2 \text{ for } E_s/N_0 \gg 1}
\end{aligned} \tag{2.4.4}$$

2.4.3 A Tight Bound for QAM

We can also tighten the general weak bound for QAM. At the signal points inside the constellation a symbol error occurs, if the received signal is outside of the square around the transmitted signal; this is the case if and only if $|\nu_I|$ or $|\nu_Q|$ are greater than $\Delta_0/2 \cdot \sqrt{E_s}$. However, as can be seen from the example of 64-QAM in Figure 2.8, at the 4 corner points the decision regions are unlimited on two sides and at the other 24 outer signal points unlimited on one side. Now we can determine a simple upper bound for the symbol-error probability by constricting the decision regions of the outer signals to the decision regions of the inner signals:

$$\begin{aligned}
P_{s,\text{QAM}} &\leq P\left(|\nu_I| > \frac{\Delta_0}{2}\sqrt{E_s} \text{ or } |\nu_Q| > \frac{\Delta_0}{2}\sqrt{E_s}\right) \\
&= 1 - P\left(|\nu_I| < \frac{\Delta_0}{2}\sqrt{E_s} \text{ and } |\nu_Q| < \frac{\Delta_0}{2}\sqrt{E_s}\right) \\
&= 1 - P\left(|\nu_I| < \frac{\Delta_0}{2}\sqrt{E_s}\right)^2 \\
&= 1 - \left(1 - P\left(\frac{|\nu_I|}{\sigma} > \sqrt{\frac{\Delta_0^2 E_s}{2N_0}}\right)\right)^2 \\
&= 1 - \left(1 - 2Q\left(\sqrt{\frac{\Delta_0^2 E_s}{2N_0}}\right)\right)^2
\end{aligned}$$

$$= 4Q \left(\sqrt{\frac{\Delta_0^2 E_s}{2N_0}} \right) \cdot \left[1 - Q \left(\sqrt{\frac{\Delta_0^2 E_s}{2N_0}} \right) \right] \quad (2.4.5)$$

Of course this bound is really only tight for higher-leveled QAM, because then the number of inner signal points dominates. In contrast, for 2-PSK and 4-PSK considerable errors occur with this upper bound, as can be seen from the performance comparison in the following subsection.

Note: except for the factor in square brackets in (2.4.5), which is approximately 1, the tight bound for QAM is twice the tight bound for PSK in terms of equal values of Δ_0 . However, this is of little consequence, since for an equal M , almost always

$$\Delta_{0,2^M\text{-PSK}} < \Delta_{0,2^M\text{-QAM}} \quad (2.4.6)$$

according to Table 2.1, except in the case of $M = 2$ where there is equality.

2.4.4 The Exact Result for ASK

Since the conditions for ASK are simpler, we can easily calculate an exact result for the symbol-error rate. For both the outer signals of 2^M -ASK,

$$P_{s,\text{outer}} = P \left(\nu > \frac{\Delta_0}{2} \sqrt{E_s} \right) \quad (2.4.7)$$

and for the $2^M - 2$ inner signals

$$P_{s,\text{inner}} = P \left(|\nu| > \frac{\Delta_0}{2} \sqrt{E_s} \right) = 2 \cdot P \left(\nu > \frac{\Delta_0}{2} \sqrt{E_s} \right) \quad (2.4.8)$$

and therefore

$$\begin{aligned} P_{s,2^M\text{-ASK}} &= \frac{1}{2^M} \left(2 \cdot P_{s,\text{outer}} + (2^M - 2) \cdot P_{s,\text{inner}} \right) \\ &= \frac{2(2^M - 1)}{2^M} \cdot P \left(\nu > \frac{\Delta_0}{2} \sqrt{E_s} \right). \end{aligned}$$

As in (2.4.5), $E(\nu^2) = N_0/2$ leads to a general exact result for arbitrary M , to the already known result for $M = 1$ and to a very precise approximation for $M \gg 1$:

$$P_{s,2^M\text{-ASK}} = \frac{2(2^M - 1)}{2^M} \cdot Q \left(\sqrt{\frac{\Delta_0^2 E_s}{2N_0}} \right) \quad (2.4.9)$$

$$\left\{ \begin{array}{l} = Q \left(\sqrt{\frac{2E_s}{N_0}} \right) \quad \text{for } M = 1 \\ \approx 2Q \left(\sqrt{\frac{\Delta_0^2 E_s}{2N_0}} \right) \quad \text{for } M > 1 \end{array} \right\}. \quad (2.4.10)$$

In (2.3.4) and (2.3.8), we had obtained

$$\Delta_{0,2^M\text{-ASK}} = \sqrt{\frac{12}{2^{2M}-1}}, \quad \Delta_{0,2^M\text{-QAM}} = \sqrt{\frac{6}{2^M-1}},$$

so for uncoded signaling with reference to E_b/N_0 ,

$$P_{s,2^M\text{-ASK}} \approx 2Q \left(\sqrt{\frac{6}{2^{2M}-1} \cdot M \cdot \frac{E_b}{N_0}} \right) \quad (2.4.11)$$

$$P_{s,2^M\text{-QAM}} \approx 4Q \left(\sqrt{\frac{3}{2^{2M}-1} \cdot 2M \cdot \frac{E_b}{N_0}} \right), \quad (2.4.12)$$

where (2.4.12) is determined from (2.4.5). Except for the factor 2 the symbol-error rates of 2^M -ASK and 2^{2M} -QAM are identical. A graphical comparison of ASK and QAM will follow in Figure 3.13.

2.4.5 Numerical Performance Results

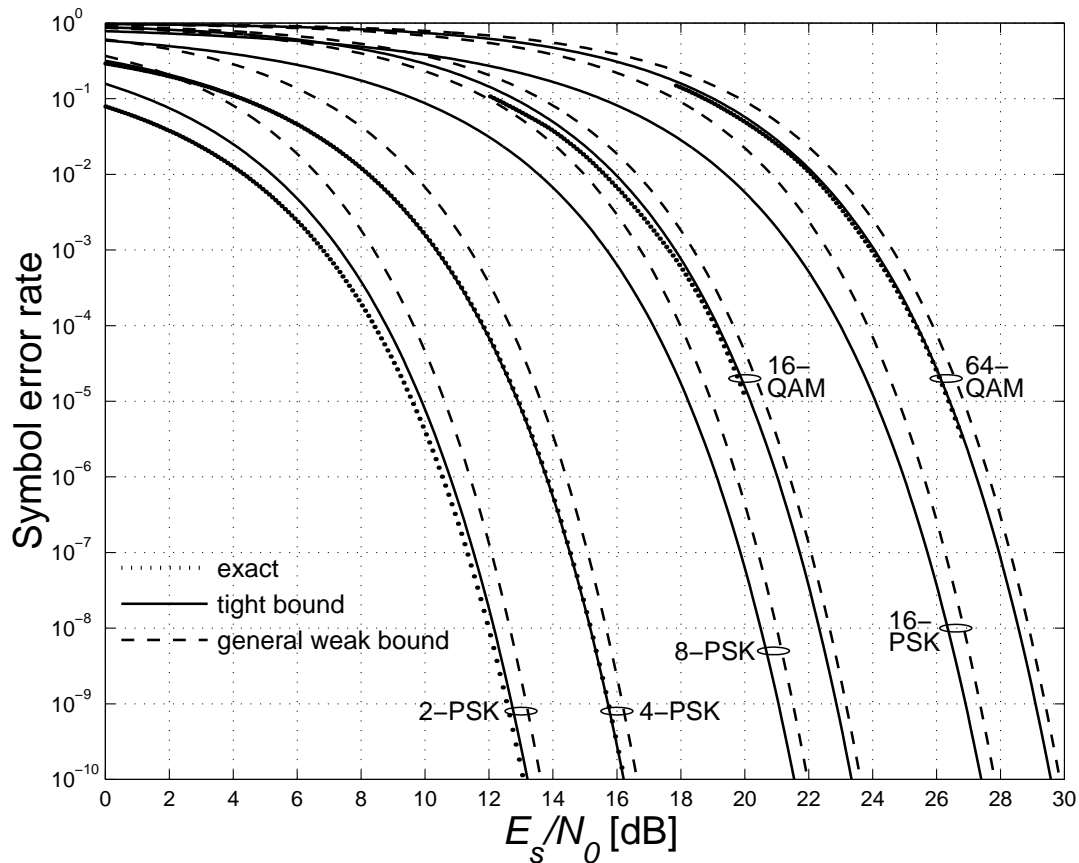


Figure 2.10. Performance of uncoded PSK and QAM over symbol energy

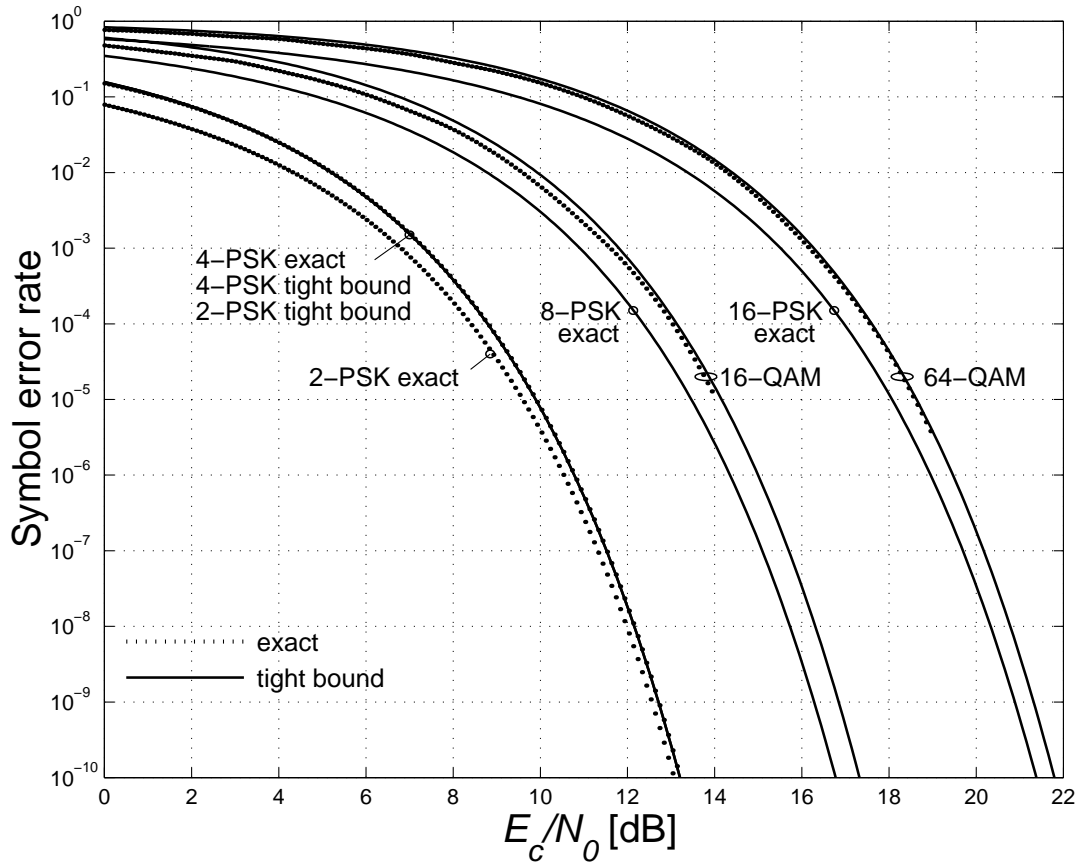


Figure 2.11. Performance of uncoded PSK and QAM over bit energy

The results derived previously are summarized as a compendium of formulas in Table 2.2, and shown as performance curves for 2-PSK, 4-PSK, 8-PSK, 16-PSK as well as 16-QAM and 64-QAM, each for the energy per symbol in Figure 2.10 and for the energy per bit in Figure 2.11. Since 2-PSK and 2-ASK as well as 4-PSK and 4-QAM are completely identical modulation schemes, these two cases are addressed as PSK schemes. In Figures 2.10 and 2.11 the tight bounds are shown with solid lines for PSK and QAM, and the exact symbol-error rate is shown with dotted lines for 2-PSK and 4-PSK (analytical results) and for 16-QAM and 64-QAM (as obtained from computer simulations). The exact symbol-error rate for 8-PSK and 16-PSK (as obtained from computer simulations) is within the line width of the concerned graphs for the tight bounds. In Figure 2.10, there is also the general weak bound sketched with dashed lines for all modulation schemes.

Generally, the difference between the tight bounds for PSK or QAM and the general weak bound in Figure 2.10 is relatively small. The vertical difference in the symbol-error rate P_s is limited to a factor of 10, and the horizontal difference in E_s/N_0 is limited to a maximum of 0.5 dB for the area below $P_s = 10^{-8}$.

The quality of the tight bounds is demonstrated by their deviation from

Table 2.2. Summary of bounds on the uncoded symbol-error rate P_s

	2^M -ary modulation scheme (ASK, PSK, QAM, arbitrary)	2-PSK ($\Delta_0 = 2$)	4-PSK ($\Delta_0 = \sqrt{2}$)
Exact results	For ASK: $\frac{2(2^M - 1)}{2^M} \cdot Q\left(\sqrt{\frac{\Delta_0^2 E_s}{2N_0}}\right),$ $\Delta_{0,\text{ASK}} \approx \sqrt{\frac{12}{2^{2M} - 1}}$ For PSK and QAM: not available	$Q\left(\sqrt{\frac{2E_s}{N_0}}\right)$	$Q\left(\sqrt{\frac{E_s}{N_0}}\right) \cdot$ $\left[2 - Q\left(\sqrt{\frac{E_s}{N_0}}\right)\right]$
Tight PSK bound	$2Q\left(\sqrt{\frac{\Delta_0^2 E_s}{2N_0}}\right),$ $\Delta_{0,\text{PSK}} = 2 \sin(\pi/2^M)$	$2Q\left(\sqrt{\frac{2E_s}{N_0}}\right)$	$2Q\left(\sqrt{\frac{E_s}{N_0}}\right)$
Tight QAM bound	$4Q\left(\sqrt{\frac{\Delta_0^2 E_s}{2N_0}}\right) \cdot$ $\left[1 - Q\left(\sqrt{\frac{\Delta_0^2 E_s}{2N_0}}\right)\right],$ $\Delta_{0,\text{QAM}} \approx \sqrt{\frac{6}{2^{2M} - 1}}$	$4Q\left(\sqrt{\frac{2E_s}{N_0}}\right) \cdot$ $\left[1 - Q\left(\sqrt{\frac{2E_s}{N_0}}\right)\right]$ not ingenious	$4Q\left(\sqrt{\frac{E_s}{N_0}}\right) \cdot$ $\left[1 - Q\left(\sqrt{\frac{E_s}{N_0}}\right)\right]$ not ingenious
General weak bound	$\exp\left(-\frac{\Delta_0^2 E_s}{4N_0}\right)$	$\exp\left(-\frac{E_s}{N_0}\right)$	$\exp\left(-\frac{E_s}{2N_0}\right)$

the exact symbol-error rates for the cases of 2-PSK and 4-PSK. For 2-PSK the deviation is fairly small; according to Table 2.2 the tight PSK bound has an error of a factor of 2. However, for 4-PSK the tight bound is very exact, as can be seen in Table 2.2 as well as in Figure 2.10 where the tight bound can not even be distinguished from the exact curve. Further computer simulations of the symbol-error rate show only small deviations for QAM and extremely small deviations for PSK from the tight bounds. So, for most practical applications and for all modulation schemes except 2-PSK, the tight bounds can be considered

as approximately exact results.

The relations between the energies for of 2^M -ary modulation schemes are reproduced from (1.4.10) to (1.4.12) for convenience:

$$\begin{aligned} E_b &= \text{energy per information bit} \\ E_c = R \cdot E_b &= \text{energy per encoded bit} \\ E_s = M \cdot E_c = RM \cdot E_b &= \text{energy per modulation symbol.} \end{aligned}$$

The modulation symbols correspond to the AWGN channel uses. Of course, $E_b = E_c$ for uncoded signaling with $R = 1$, and $E_c = E_s$ for coded binary modulation with $M = 1$.

With reference to E_s/N_0 there is a difference of 3 dB between 2-PSK and 4-PSK, with reference to E_b/N_0 the uncoded symbol-error rates of both modulation schemes only differ by a factor of 2 because

$$P_{s,4\text{-PSK}} \approx 2 \cdot Q\left(\sqrt{\frac{2E_c}{N_0}}\right) = 2 \cdot P_{s,2\text{-PSK}}. \quad (2.4.13)$$

The reason for this is fairly simple. Since the inphase and quadrature phase of 4-PSK are statistically independent, one 4-PSK signal is equivalent to two consecutive 2-PSK signals. The bit-error rates P_b of 2-PSK and 4-PSK are actually identical in reference to E_c/N_0 as will now become clear.

2.4.6 Gray Code Mapping

The relation between the symbol-error rate P_s and the bit-error rate P_b for an arbitrary 2^M -ary modulation scheme is

$$\frac{P_s}{M} \leq P_b \leq P_s, \quad (2.4.14)$$

since an incorrect demodulation of the symbol results in between 1 and M bit errors. Usually $M/2$ bits are affected in the case of a symbol error [128], so that

$$P_b \approx \frac{1}{2} \cdot P_s \quad (\text{general mapping}). \quad (2.4.15)$$

However, the mapping of the M bits to the 2^M possible modulation symbols may be done in a number of ways. The best assignment is a widely-used mapping known as *Gray coding* [114, 127], where adjacent points in the signal constellation only differ in one bit. The Gray code mapping can be applied to all ASK, PSK and QAM signal constellations, and is demonstrated for the examples of 8-PSK and 16-QAM in Figure 2.12 and for 8-ASK in Figure 10.10.

For Gray code mapping at large signal-to-noise ratios, we can assume that the most likely symbol errors are caused by the erroneous selection of an adjacent

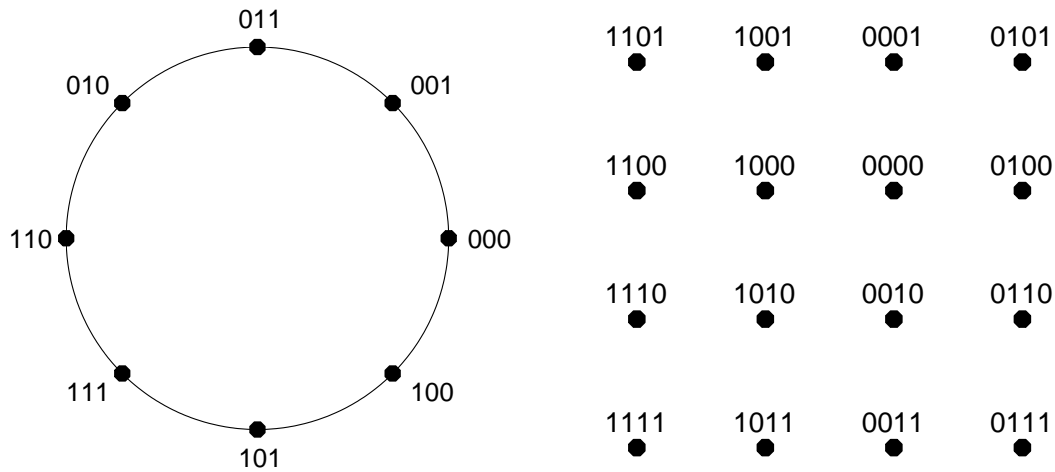


Figure 2.12. Gray code mappings for 8-PSK and 16-QAM

amplitude to the transmitted signal amplitude. In such a case, only a single bit error occurs for the 2^M -ary symbol, so that

$$P_b \approx \frac{1}{M} \cdot P_s \quad (\text{Gray code mapping}). \quad (2.4.16)$$

This approximation is also contained in the more general result (1.3.19), where $P_b = p_{e,\text{abstract}}$ with $q = 2$ and $P_s = p_{e,\text{inner}}$.

The exact performance curves for the bit-error rate P_b of uncoded PSK and QAM with Gray code mapping (obtained by computer simulation, and for PSK also listed in [127]) are shown in Figure 2.13, where the difference to the symbol-error rate P_s (represented by the tight bounds from Figure 2.11) is actually about a factor of M .

2.4.7 Spectral Efficiency

The comparisons of digital modulation schemes in Figures 2.10, 2.11 and 2.12 on the basis of the required signal-to-noise ratio, to achieve a specified error rate, are interesting and reflect all essential aspects for the performance of a modulation scheme. However, it is important to emphasize in particular the very different throughput depending on the number of modulation levels in a further comparison.

As in Chapter 1, let R be the code rate (in units of information bits per encoded bit), r_b be the information bit rate (in units of information bits per second), and $r_s = r_b/(RM)$ be the symbol rate or baud rate (in units of 2^M -ary modulation symbols per second) according to (1.4.6). The ratio $r_b/W = RM \cdot r_s/W$ of the information bit rate to the bandwidth is called *spectral efficiency*, *spectral bit rate* or *bandwidth efficiency* in units of information bits per second per Hertz (see also Definition 3.5). Assume the minimum Nyquist bandwidth,

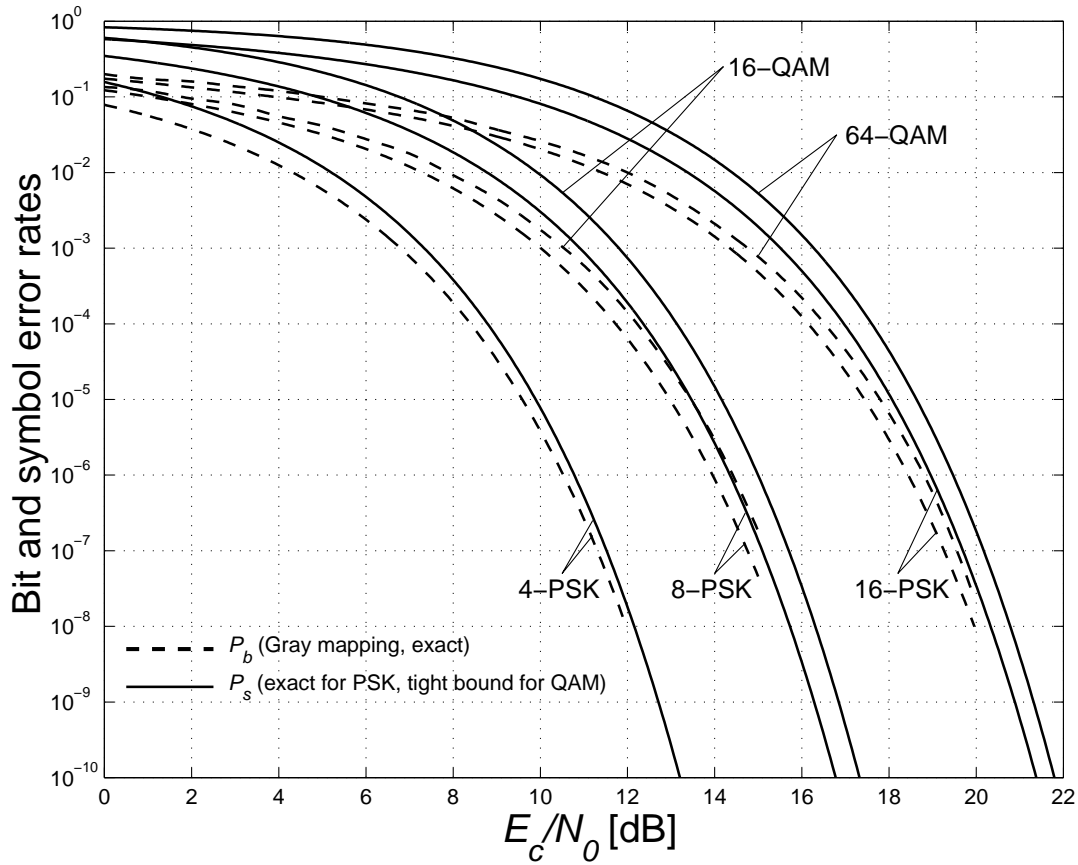


Figure 2.13. Bit-error rate with Gray code mapping and symbol-error rate of uncoded PSK

then (2.2.19) implies that

$$\frac{r_b}{W} = \left\{ \begin{array}{ll} 2M & \text{for baseband channels} \\ M & \text{for passband channels} \end{array} \right\} \quad (2.4.17)$$

in case of uncoded signaling with $R = 1$.

A compact and meaningful comparison of different digital modulation schemes could be based on the spectral efficiency or simply on M versus the signal-to-noise ratio E_b/N_0 which is required to achieve a given bit-error rate. Such a representation is given in the next chapter in Figure 3.11 together with the Shannon capacity boundary. Yet, QAM still proves to be more efficient than PSK: for equal E_b/N_0 , QAM provides higher spectral efficiency, and for equal spectral efficiency and equal symbol-error rate QAM requires less E_b/N_0 than PSK. However, a practical disadvantage of QAM is that it reacts much more sensitively to non-linearities in the transmitter and receiver amplifiers than PSK does. The considerations on spectral efficiencies will be continued in Subsection 3.5.2 as well as in Chapter 11.

2.5 Asymptotic Coding Gains for 2^M -ary Modulation Schemes

2.5.1 Uncoded Signaling

In the previous section we discussed symbol-error rates and bit-error rates. Particularly for higher error probabilities, say $P_s > 10^{-5}$, it is not only the distance and the number of the nearest neighbours which are important, but also the neighbours which are a little further away.

In this section we will inspect the asymptotic differences in E_s/N_0 as $E_s/N_0 \rightarrow \infty$. This corresponds to a situation with very small error probabilities, say $P_s < 10^{-5}$. The asymptotic behaviour is exclusively determined by the distance of the nearest neighbour to the transmitted signal and therefore solely by the value of the minimum Euclidean distance Δ_0 . For QAM the outer decision regions are unlimited in one or two directions and for PSK the decision regions have the form of unlimited sectors, but asymptotically this is of no importance. Moreover, the exact results, the tight bounds and the weak bounds are asymptotically identical.

If an arbitrary modulation scheme (denoted by the index “mod” in the following) is to attain the same error rate as 2-PSK, then asymptotically, according to the last row in Table 2.2, as $E_s/N_0 \rightarrow \infty$

$$\exp\left(-\frac{\Delta_{0,\text{mod}}^2}{4} \left(\frac{E_s}{N_0}\right)_{\text{mod}}\right) = \exp\left(-\left(\frac{E_s}{N_0}\right)_{2\text{-PSK}}\right).$$

Thus for the necessary additional E_s/N_0 in comparison to 2-PSK, expressed in decibels,

$$\left(\frac{E_s}{N_0}\right)_{\text{mod}} - \left(\frac{E_s}{N_0}\right)_{2\text{-PSK}} = 10 \cdot \log_{10} \left(\frac{4}{\Delta_{0,\text{mod}}^2}\right) \text{ dB}. \quad (2.5.1)$$

These values are shown in Figure 2.14. Similarly, for E_c/N_0 , and shown in Figure 2.15,

$$\left(\frac{E_c}{N_0}\right)_{\text{mod}} - \left(\frac{E_c}{N_0}\right)_{2\text{-PSK}} = 10 \cdot \log_{10} \left(\frac{4}{M \cdot \Delta_{0,\text{mod}}^2}\right) \text{ dB}. \quad (2.5.2)$$

Obviously, a linear increase of the spectral efficiency M also calls for an approximate linear increase of E_s/N_0 . An increase of the spectral efficiency M by 1 bit/s/Hz with a fixed symbol-error rate can be compensated for by increasing E_s/N_0 by a factor of about

- 4 (corresponds to 6 dB) for PSK and ASK, or
- 2 (corresponds to 3 dB) for QAM.

The values in Figures 2.14 and 2.15 can also be approximately derived from Figures 2.10 and 2.11 at $P_s = 10^{-10}$ as well as from Figure 3.11 with the relation $E_s = M \cdot E_c$ for the uncoded transmission we are considering here.

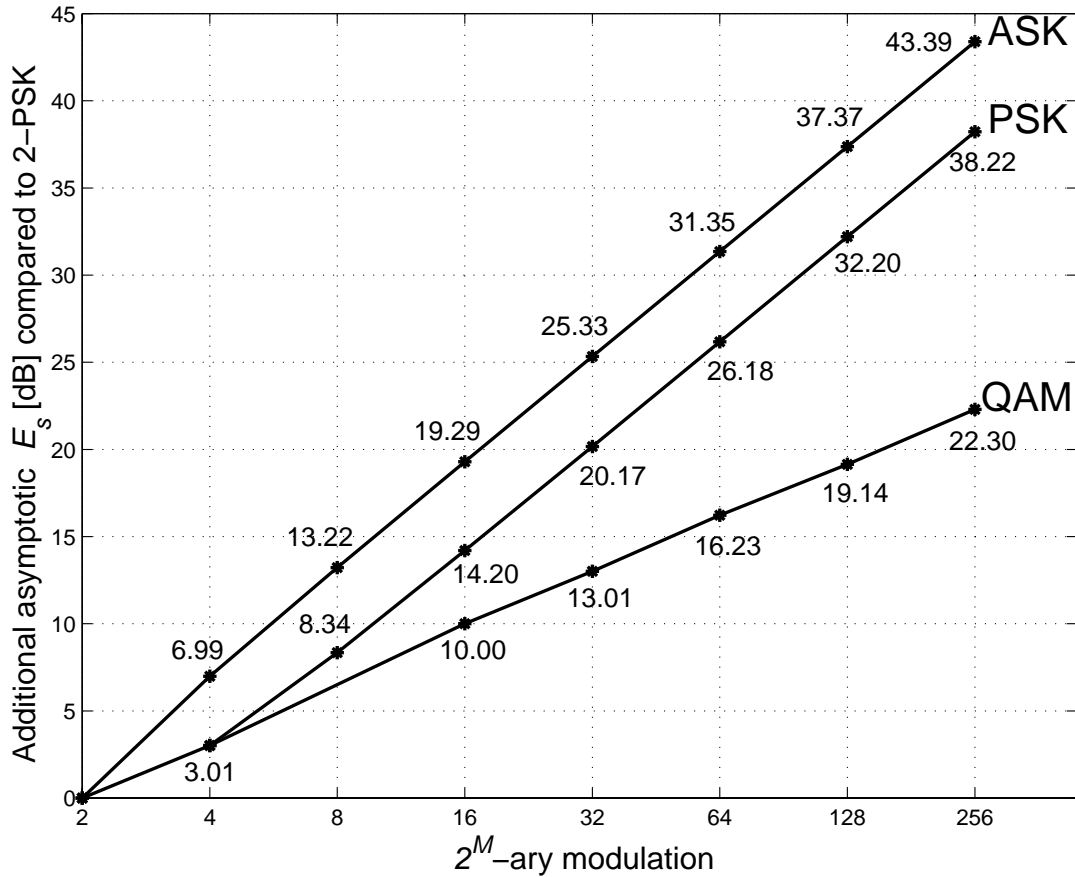


Figure 2.14. Additional E_s/N_0 [dB] required for 2^M -ary modulation compared to binary modulation (asymptotically for $E_s/N_0 \rightarrow \infty$)

2.5.2 Coded Signaling

We will now extend the considerations on asymptotic coding gains for binary communication in Section 1.7 to 2^M -ary modulation methods.

First, we assume hard-decision demodulation. Except for asymptotically uninteresting factors, the bit-error or symbol-error probability after demodulation (and thus prior to decoding) is, according to Table 2.2,

$$p_e = \text{const} \cdot Q \left(\sqrt{\frac{\Delta_0^2 E_s}{2N_0}} \right), \quad (2.5.3)$$

where $E_s = RM \cdot E_b$. The result (1.3.15) for the binary case is again obtained from (2.5.3) by applying $\Delta_0 = 2$, $M = 1$ and $E_c = RE_b$. Now we insert p_e from

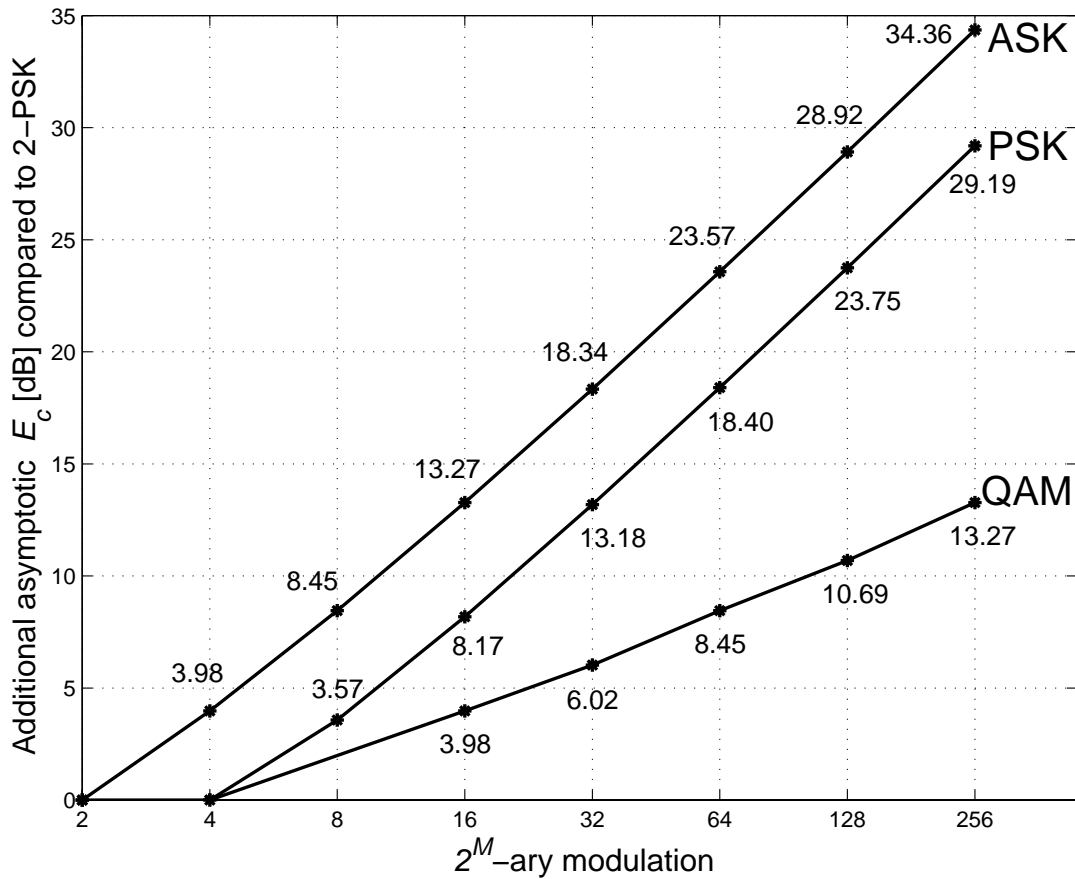


Figure 2.15. Additional E_c/N_0 [dB] required for 2^M -ary modulation compared to binary modulation (asymptotically for $E_c/N_0 \rightarrow \infty$)

(2.5.3) in equation (1.7.5) to obtain the post-decoding word-error probability P_w

$$P_w = \text{const} \cdot p_e^{t+1} \quad (2.5.4)$$

$$= \text{const} \cdot Q \left(\sqrt{\frac{\Delta_0^2(t+1)}{2} \cdot \frac{E_s}{N_0}} \right) \quad (2.5.5)$$

$$= \text{const} \cdot Q \left(\sqrt{\frac{\Delta_0^2(t+1)RM}{2} \cdot \frac{E_b}{N_0}} \right), \quad (2.5.6)$$

where $t = \lfloor (d_{\min} - 1)/2 \rfloor$. Thus the asymptotic coding gain for hard decisions, defined as the asymptotic gap between coded 2^M -ary and uncoded 2^M -ary modulation, with respect to E_b/N_0 , is independent of M :

$$G_{a,\text{hard}} = 10 \cdot \log_{10}((t+1)R) \quad \text{dB}. \quad (2.5.7)$$

The asymptotic coding gain, with respect to E_s/N_0 , is additionally also independent of R :

$$G_{a,\text{hard}}^* = 10 \cdot \log_{10}(t+1) \quad \text{dB}. \quad (2.5.8)$$

For soft-decision demodulation $t + 1$ is to be replaced by d_{\min} . For completeness, note that for the convolutional codes introduced in Chapters 9 and 10 $t + 1$ in (2.5.7) and (2.5.8) have to be replaced by $d_f/2$ for hard decisions and d_f for soft decisions (see Theorem 10.1).

These asymptotic relations are summarized in Figure 2.16. The differences between coded and uncoded signaling are independent of M . Of course, the difference between binary and high-level modulation schemes depends considerably on M and the curves for 2^M -ary modulation shift to the right for increasing M . However, Subsection 10.3.3 will show that coded 2^M -ary modulation performs much better in practice for relevant error rates than suggested by the asymptotic gaps, i.e., the curve for coded 2^M -ary modulation shifts a little to the left in Figure 2.16.

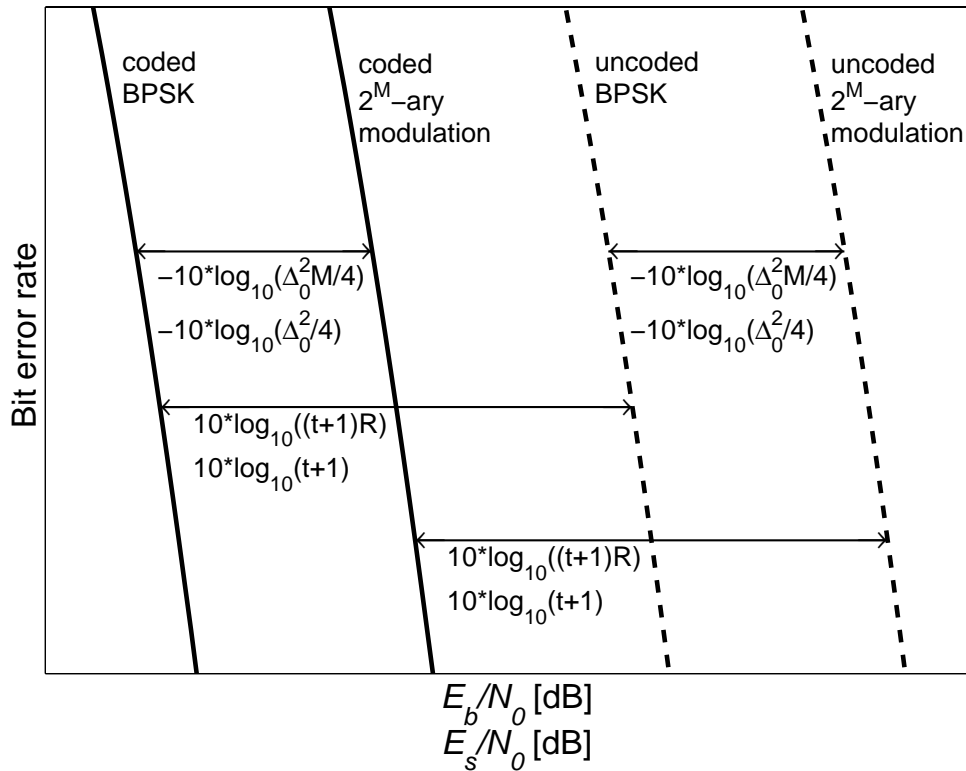


Figure 2.16. Asymptotic gaps between coded and uncoded 2^M -ary modulation schemes (upper values refer to E_b/N_0 , lower values refer to E_s/N_0)

Finally, the gap between 2^M -ary coded modulation and uncoded BPSK is $10 \cdot \log_{10}(M\Delta_0^2 \cdot (t + 1)R/4)$ in decibels with respect to E_b/N_0 . This value can also be negative for high-level modulation and weak coding schemes, in which case, in contrast to Figure 2.16, the graph for uncoded BPSK lies to the left of the graph for coded 2^M -ary modulation.

Example 2.2. Let us consider a transmission with 16-QAM and a symbol-error rate of $P_s = 10^{-8}$ to illustrate the relations in Figure 2.16. For uncoded

16-QAM transmission we obtain about $E_b/N_0 = 16.0$ dB according to Figure 2.13. Uncoded BPSK requires $E_b/N_0 = 12.0$ dB according to Table 1.1, so there is a difference of about 4.0 dB between uncoded BPSK and uncoded 16-QAM, which corresponds nicely to the value of 3.98 dB in Figure 2.15.

We will now assume a coding scheme with rate $R = 1/2$ and a coding gain of $G_a = 6.2$ dB with reference to E_b/N_0 at $P_s = 10^{-8}$ for soft-decision demodulation. For a realistic example we refer to the convolutional code with a memory length of $m = 6$ in Figure 10.7, where the application of coding reduces the required E_b/N_0 from 12.0 dB to 5.8 dB for BPSK. According to Figure 2.16, coding for 16-QAM again saves 6.2 dB and we expect the required E_b/N_0 to be reduced from 16.0 dB to 9.8 dB. However, as we will see in Subsection 10.3.3, only about 8.5 dB are required. ■

In contrast to the comparison between coded and uncoded transmission for identical modulation schemes, which should be made with reference to E_b/N_0 , the comparison for trellis coded modulation (TCM), as discussed in Chapter 11, can also be made with reference to E_s/N_0 , since the coding incorporated with TCM neither changes the symbol rate and thus the bandwidth nor the throughput defined by the information bit rate r_b .

2.6 Summary of the Most Important Parameters for Coded AWGN Channels

The most important parameters describing a coded transmission over the AWGN channel including its physical units are summarized in Table 2.3. For completeness the channel capacity is also mentioned in Table 2.3, which will be introduced in the following Chapter.

The most important relations between the parameters in Table 2.3 are recapitulated below. For the code rate and the rates of the information bits, encoded bits and modulation or channel symbols,

$$R = \frac{k}{n}, \quad R_q = R \cdot \log_2 q, \quad R_M = RM, \quad (2.6.1)$$

$$r_c = \frac{r_b}{R}, \quad r_s = \frac{r_c}{M} = \frac{r_b}{RM} = \frac{1}{T_s}. \quad (2.6.2)$$

For the minimum Nyquist bandwidth W , attained for a rolloff factor of $\alpha = 0$,

$$W = \left\{ \begin{array}{ll} r_s/2 & \text{baseband channel} \\ r_s & \text{passband channel} \end{array} \right\}. \quad (2.6.3)$$

In more detail, the transmitted signal is restricted to frequencies f defined by

$$\left\{ \begin{array}{ll} |f| < W = r_s/2 & \text{baseband channel} \\ |f \pm f_c| < W/2 = r_s/2 & \text{passband channel} \end{array} \right\}. \quad (2.6.4)$$

Table 2.3. Important parameters of coded AWGN channels and their units

Parameter	Name	Physical units
R	code rate	info bit/encoded bit
R_q	code rate	info bit/ q -ary encoded symbol
R_M	code rate	info bit/ 2^M -ary modulation symbol
r_b	info bit rate (throughput)	info bit/second
r_c	encoded bit rate	encoded bit/second
r_s	symbol rate (baud rate)	2^M -ary modulation symbol/second
T_s	symbol duration	second
W	bandwidth	Hertz
r_b/W	spectral efficiency	info bit/second/Hertz
E_b	energy per information bit	Joule = Watt·second
E_c	energy per encoded bit	Joule
E_s	energy per mod.symbol	Joule
S	signal power	Watt
N_0	one-sided noise power density	Joule = Watt/Hertz
N	noise power	Watt
C	channel capacity	info bit/(2^M or q)-ary symbol
C^*	channel capacity	info bit/second
C^*/W	capacity boundary on r_b/W	info bit/second/Hertz

For the spectral efficiency of 2^M -ary modulation,

$$\frac{r_b}{W} = RM \cdot \frac{r_s}{W} = \begin{cases} 2RM & \text{baseband channel} \\ RM & \text{passband channel} \end{cases}. \quad (2.6.5)$$

We assume the AWGN channel with $y = x + \nu$. For the signal energy,

$$E_c = R \cdot E_b, \quad E_s = E(|x|^2) = M \cdot E_c = RM \cdot E_b, \quad (2.6.6)$$

and for the signal power

$$S = E_s \cdot r_s = E_c \cdot r_c = E_b \cdot r_b, \quad (2.6.7)$$

which are valid both for baseband and passband channels. For the noise energy, $E(\nu^2) = N_0/2$ for baseband signaling and $E(|\nu|^2) = E(|\nu_I|^2) + E(|\nu_Q|^2) = N_0/2 + N_0/2 = N_0$ for passband signaling. For the noise power,

$$N = N_0 \cdot W = \begin{cases} N_0 \cdot r_s/2 & \text{baseband channel} \\ N_0 \cdot r_s & \text{passband channel} \end{cases}, \quad (2.6.8)$$

and for the signal-to-noise ratio

$$\frac{S}{N} = \frac{E(|x|^2)}{E(|\nu|^2)} = \begin{cases} 2 \cdot E_s/N_0 & \text{baseband channel} \\ E_s/N_0 & \text{passband channel} \end{cases}. \quad (2.6.9)$$

In Chapter 3, we will introduce the channel capacity, and we have the relation $C^* = C \cdot r_s$ for the connection between the reference to seconds and to 2^M -ary modulation symbols. The corresponding relation is $r_b = R_M \cdot r_s$. The

Shannon Noisy Channel Coding Theorem 3.1 and the Shannon-Hartley Theorem 3.5 provide the boundaries $R_M < C$ and $r_b < C^*$ for the maximum code rate and the maximum throughput. The Shannon-Hartley Theorem 3.5 together with

$$\frac{r_b}{W} < \frac{C^*}{W} = \log_2 \left(1 + \frac{S}{N} \right) \quad (2.6.10)$$

provides us with a capacity boundary for the spectral efficiency.

2.7 Problems

- 2.1.** Derive the matched filter for the baseband AWGN channel: let $h_{Tx}(t)$ be the transmitter filter and $h_{Rx}(t)$ be the receiver filter. Prove that the received signal-to-noise energy takes on its maximum if $h_{Rx}(t) = h_{Tx}(-t)$. Hint: apply Schwarz's inequality as stated in (A.1.9).
- 2.2.** Show that the path loss for a C-band (6 GHz) link of a synchronous altitude satellite is about 200 dB.
- 2.3.** Consider a microwave line-of-sight link for a wireless broadband access system. The carrier frequency is 26 GHz with rain fading of 5 dB per km, the symbol rate is 20 Msample/s, and the range is 4 km. Assume a base station with a transmit power of 20 dBm and an antenna gain of 17 dBi (45 degree sectorization) and a link margin of 3 dB.

Which diameter of a parabolic antenna at the fixed terminal station (assume an antenna efficiency of 0.5 and a noise figure of 8 dB) is required to guarantee a bit-error rate of 10^{-10} in the case of uncoded binary PSK?

